12-2014

Comparative Analysis of Clavicular Tunnel Configuration for Coracoclavicular Ligament Reconstruction

Mark Omwansa
Western Michigan University, m.omwansa@gmail.com

COMPARATIVE ANALYSIS OF CORACOCLAVICULAR LIGAMENT RECONSTRUCTION

by

Mark Omwansa

A thesis submitted to the Graduate College
in partial fulfillment of the requirements
for the degree of Master of Science in Engineering (Mechanical)
Mechanical and Aeronautical Engineering
Western Michigan University
December 2014

Thesis Committee:

Peter Gustafson, Ph.D., Chair
James Kamman, Ph.D.
Andrew Geeslin, M.D.

COMPARATIVE ANALYSIS OF CLAVICULAR TUNNEL CONFIGURATION FOR CORACOCLAVICULAR LIGAMENT RECONSTRUCTION

Mark Omwansa, M.S.E.

Western Michigan University, 2014

A number of coracoclavicular ligament reconstructions are carried out each year and post surgical fractures of the clavicle have been reported. The primary objective of this research is to develop a comparative metrics that compares clavicular tunnel configurations used in coracoclavicular reconstruction techniques. The goal of this comparison is to reduce post surgical failures due to clavicle fractures. The present analysis compared two techniques – a single 3 mm clavicular tunnel and the other double 6 mm tunnels – experimentally, using Four-point bending testing and Finite Element Analysis (FEA). A unique method, slicing, was used to create an FE clavicle mesh model. This model was validated and used for the simulations. The FE models' location of maximum principal stress correlated with experimental failure locations in both clavicle groups. Testing results show CC reconstruction techniques with single 3 mm tunnels result in a clavicle that is stronger and stiffer than techniques with two 6 mm tunnels.

ACKNOWLEDGMENTS

I would like to thank my mom, grandparents, aunts and uncles for their prayers, guidance and continued support throughout the years. This academic achievement is a testament of the great job and resilience they have shown in raising me as child until now. I would also like to thank my committee: Professor Peter Gustafson, Professor James Kamman, Dr Andrew Geeslin and Mr. Glen Hall for guiding me and being great mentors to me through my Master's career. Lastly, but not least, I want to thank my friends and lab partners that helped and lightened this tenuous load of getting a Master's degree.

Mark Omwansa

Contents

List of Tables

List of Figures

Chapter 1

Introduction

Injuries to the Acromioclavicular (AC) joint make up 0"%" – 12"%" of all shoulder girdle injuries [15]. These injuries are normally caused by a direct blow to the AC joint, and are common in sports like biking, football and rugby [17]. The AC and Coracoclavicular (CC) ligaments are most susceptible to damage during these kinds of injuries. The AC and CC ligaments connect the clavicle to the scapula at the acromion and coracoid process, respectively. These two ligaments play an important role in the clavicle's stability, which supports and holds the arm and scapula in position, giving the arm a wide range of movement. The clavicle also protects vital arteries that transport blood in the upper body. The AC ligaments stabilize the clavicle horizontally at the AC joint, while the CC ligaments, the conoid and trapezoid, are responsible for vertical stability [17]. Studies have shown the CC ligaments to be stronger than the AC joint ligament with a combined strength that ranges between 500 $\pm$ 134 N to 725 $\pm$ 231 N when intact [9]. Figure 1.1 shows the bones and ligaments that make up the right shoulder girdle.

Acromioclavicular joint injuries are classified according to the Rockwood classification into six types [9] as shown in Figure 1.2 [17]. It is widely accepted that

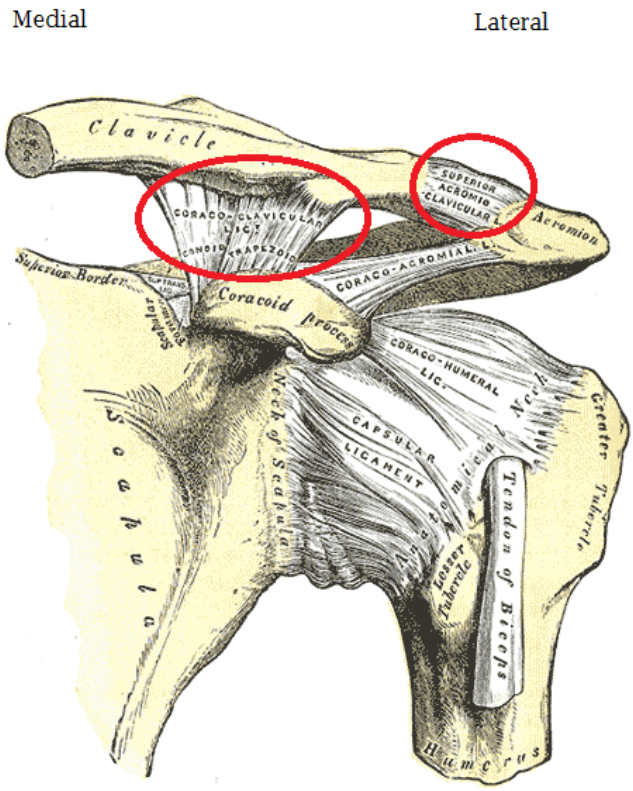

Figure 1.1: *Right Should Girdle. Circled in red: CC and AC ligaments [11]*

Types I and II injuries are treated non-surgically, while Types IV – VI are treated surgically [12]. Type III injuries can be treated either surgically or non-surgically, depending on the doctor's judgment [9].

There are over 60 recorded surgical techniques used to treat AC joint injuries [18]. The surgical technique used varies between doctors, but the literature shows that Weaver – Dunn has been one of the most popular AC repair techniques [14]. Morbidity of the CC reconstruction techniques have also been reported, including fracturing of the clavicle through reconstruction tunnels [15]. To discern the biomechanical causes of this failure mode, several quantitative comparison methods are proposed and implemented in this thesis.

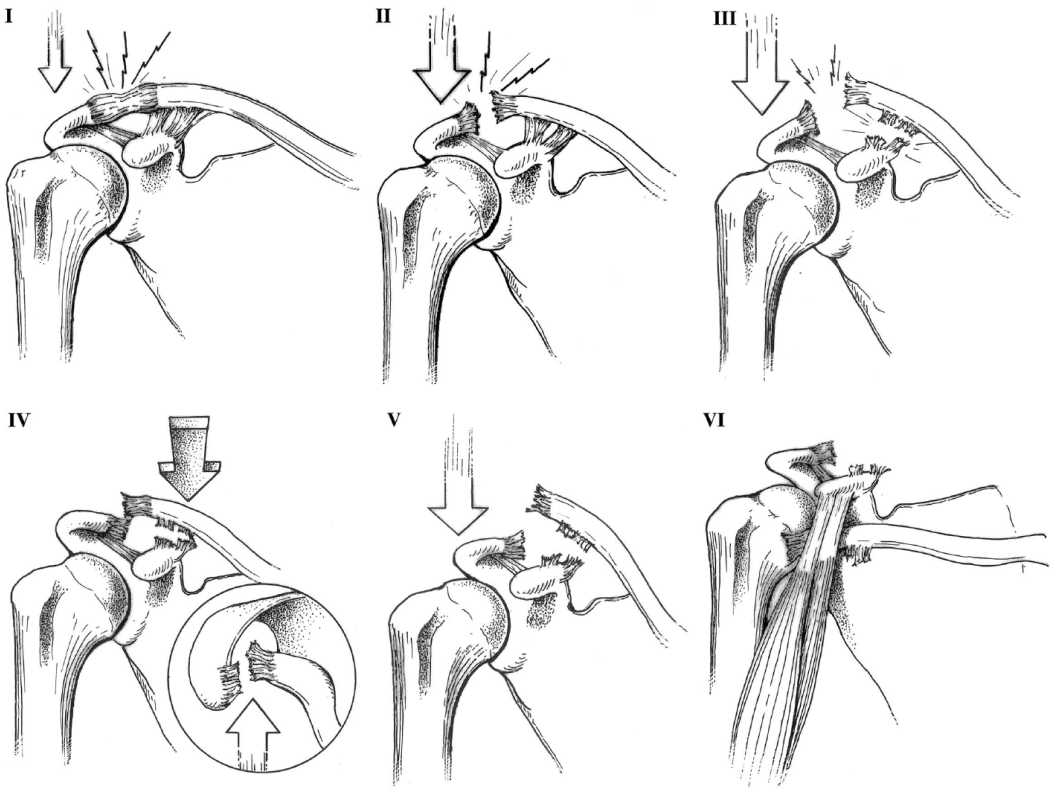

Injury type	Acromioclavicular ligament	Coracoclavicular ligament	Direction
I	Sprain	Intact	Nondisplaced
II	Complete disruption	Sprain	<25% Superior
III	Complete disruption	Complete disruption	25%–100% Superior
IV	Complete disruption	Complete disruption	Posterior through the trapezius
V	Complete disruption	Complete disruption	100%–300% Superior
VI	Complete disruption	Complete disruption	Inferior to acromion or coracoid

Figure 1.2: *Images [17] and Summary [12] of Rockwood Classification*

1.1 Surgical Techniques

Suture-button fixation and the Anatomic Coracoclavicular (CC) Reconstruction techniques, are specific examples of the one and two tunnel reconstruction techniques, which are the focus of this thesis. The tunnels are used for high-strength sutures or tendon grafts that stabilize the clavicle [6, 14]. The detailed surgical procedures described in the literature is beyond the scope of this research. The surgical summaries in this section contain information about the number of holes, their sizes, and their locations on the clavicle. The clavicle specimens tested received either single 3 mm diameter tunnel or double 6 mm diameter tunnels, two

tunnel sizes based on existing surgical techniques.

1. *Dogbone AC Repair*

   Figure 1.3 shows the Dog bone button technique, which involves drilling one 3 mm diameter tunnel in the clavicle approximately 35 mm from the acromion. Synthetic suture is then passed through the hole and held in place by titanium Dogbone buttons [6].

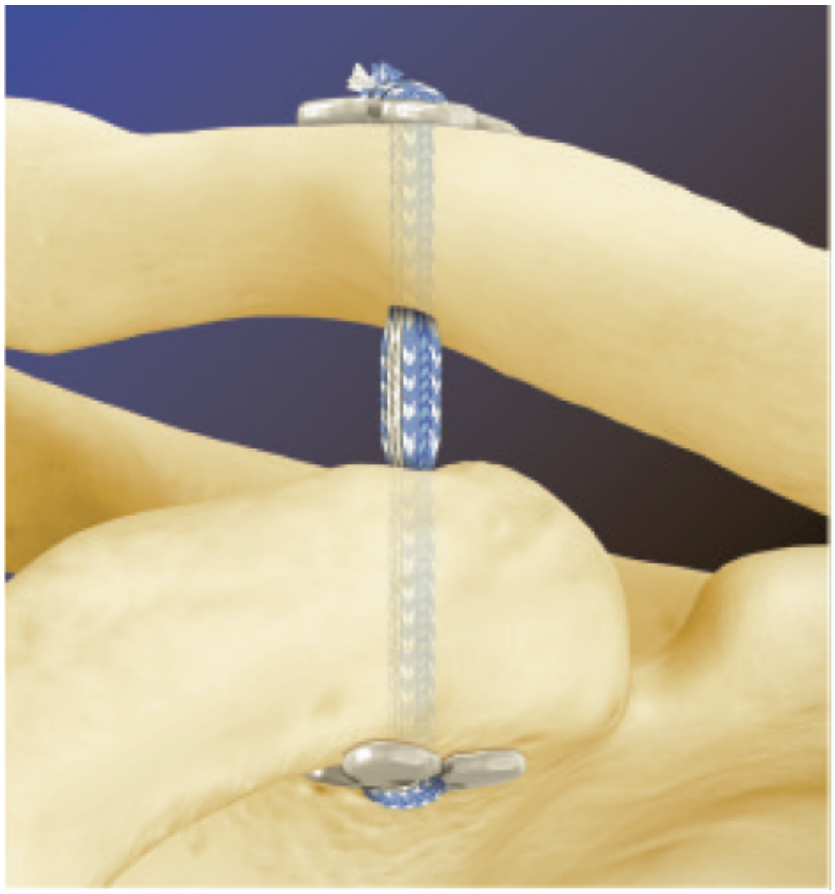

Figure 1.3: *Dogbone Technique [6]*

2. *Anatomic CC Reconstruction*

   The Anatomic CC Reconstruction Technique involves looping a tendon graft around the coracoid and securing the free ends in the clavicle using Tenodesis screws. Therefore, two tunnels are drilled into the distal clavicle at approximately 30 mm and 45 mm from the acromion. Figure 1.4 is an illustration

of a completed Anatomic CC Reconstruction.

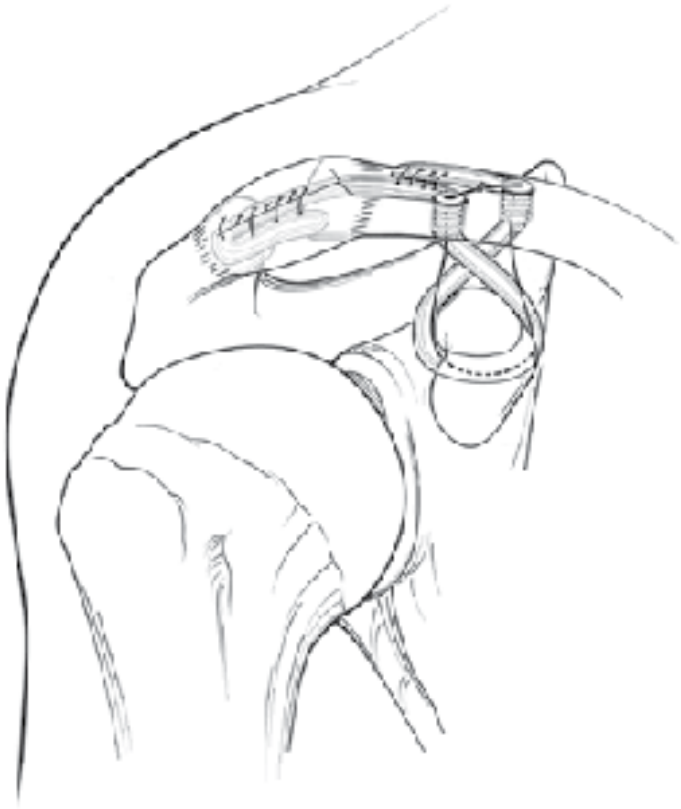

Figure 1.4: *Anatomic Reconstruction Technique [14]*

3. *Summary of Reconstruction Techniques*

   Table 1.1 summarizes the modifications on the clavicle with each surgical technique. For the purpose of this thesis, these techniques were grouped into two major groups: single and double tunnel reconstructions and techniques. Therefore, the synthetic clavicles used in experiments either received one or two tunnel through them. Using synthetic clavicles is beneficial because they have more homogeneous properties than cadaver bones [1], and they are readily available. However beneficial, the homogeneity of the synthetic

clavicle bones may not be representative of the population.

Table 1.1: *Summary of Surgical Techniques*

Surgical Technique	Number of Tunnels	Location of Tunnel/s w.r.t the Acromion	Diameter of Tunnel/s
Dog bone	1	35 mm	3 mm
Anatomic Reconstruction Techique	2	29 mm & 45 mm	6 mm

1.2 Selection of Comparison Method

Flexural testing was selected to compare the surgical techniques due to its ease in implementation and analysis. The clavicle also experiences some flexural and torsion loads during shoulder movements, which makes this kind of testing appropriate. Options for loading and boundary conditions were narrowed to three flexural tests common in biomechanics publications. The three flexural tests seen in literature are cantilever beam bending [4], simply supported three-point bending [13], and four-point bending [16].

The moment (M) and shear force (S) of these three configurations were analytically calculated and used for comparison. The primary assumption for the calculations is the clavicle satisfies Euler-Bernoulli beam criteria, which does not. It does not meet the 16:1 length-to-width ratio requirement set for Euler-Bernoulli beams [19]. However, the flexural moment and shear force were still calculated using Equations 1.1 and 1.2. Both the results and configuration are shown in Figures 1.5, 1.6 and 1.7.

The results show that simply supported four point bending has properties that make it advantageous over the other configurations. The constant moment and zero shear region in between the top, inner supports that the four point bending configuration provides are good comparison metrics. The entire length of the

clavicle will be experience a similar moment, which simplifies comparing tunnel configurations. Therefore, it was concluded that simply supported four point bending would be used to compare the surgical techniques.

$$M = EI\frac{d^2w}{dx^2} \tag{1.1}$$

$$S = EI\frac{d^3w}{dx^3} \tag{1.2}$$

1.3 Objectives and Thesis Summary

The objectives of this thesis are to develop a four point bending fixture and use it to test tunnel configurations for CC ligament reconstruction techniques, and to create an accurate Finite Element (FE) model of the clavicle that can be used in future analysis. The four point bending scenario of the clavicle was simulated by applying a moment at the acromial end while constraining the sternal end in all directions. The constraint applied to the sternal end will produce an equal and opposite reaction moment at the sternal end, and thus simulating the region of constant bending the four point bending setup.

Experimental testing and FE modeling of the clavicle, or any other bone, are not unique practices. Chapter 2 summarizes the work done by biomechanics researchers and their findings.

Chapter 3 chronicles the development of both the four point bending fixture and the FE model of the clavicle. The first section, 3.1, focuses on the experimental aspect of the thesis. In this section, there is a description of the fixture that were built for the experiment, and summary of the experimental procedures. Section 3.2 describes the activities performed to create and validate the FE model

of the clavicle.

The experimental and FE results are summarized and discussed in chapters 4 and 5, respectively. The fifth chapter will conclude with a discussions on the findings of this thesis and thoughts on future work for the research. The contributions and recommendation of the masters research are recorded in Chapter 6.

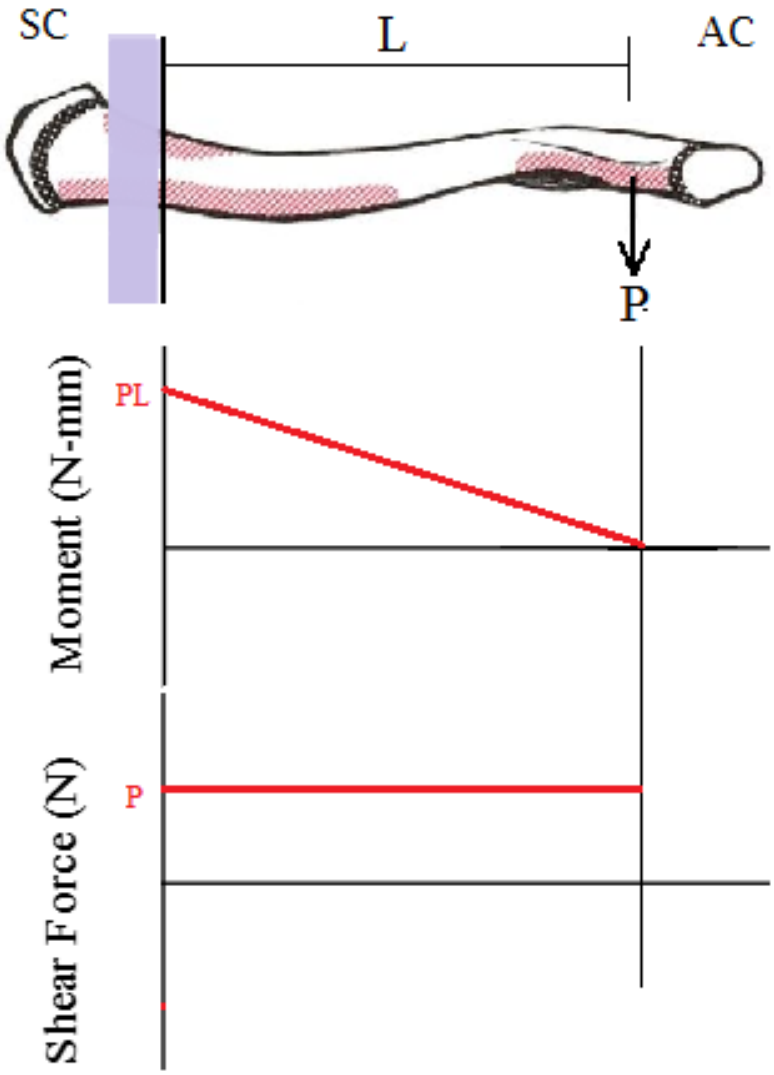

Figure 1.5: *Schematic Drawing of Cantilever beam bending with Moment and Shear Forces Through its Length*

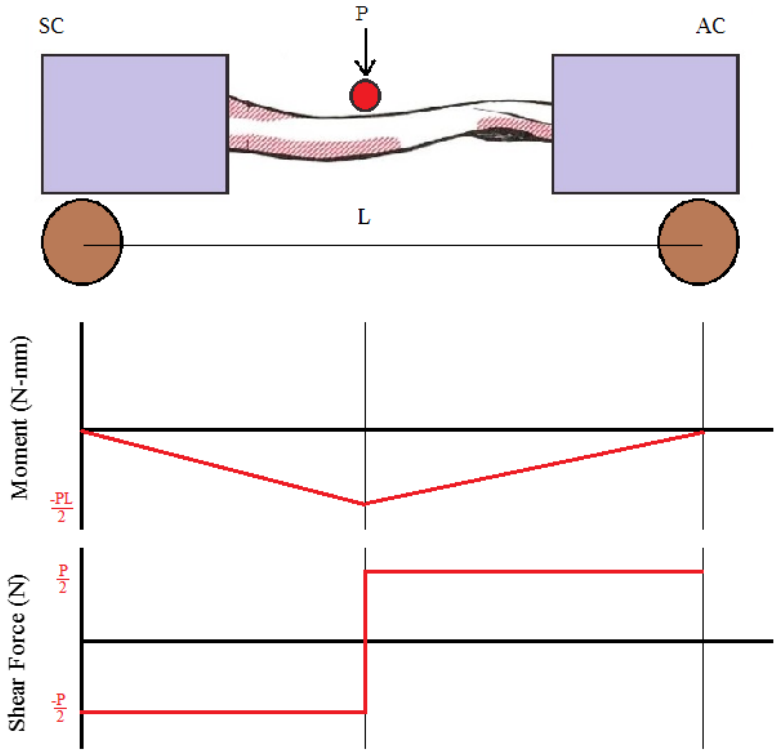

Figure 1.6: *Schematic Drawing of Three point bending with Moment and Shear Forces Through its Length*

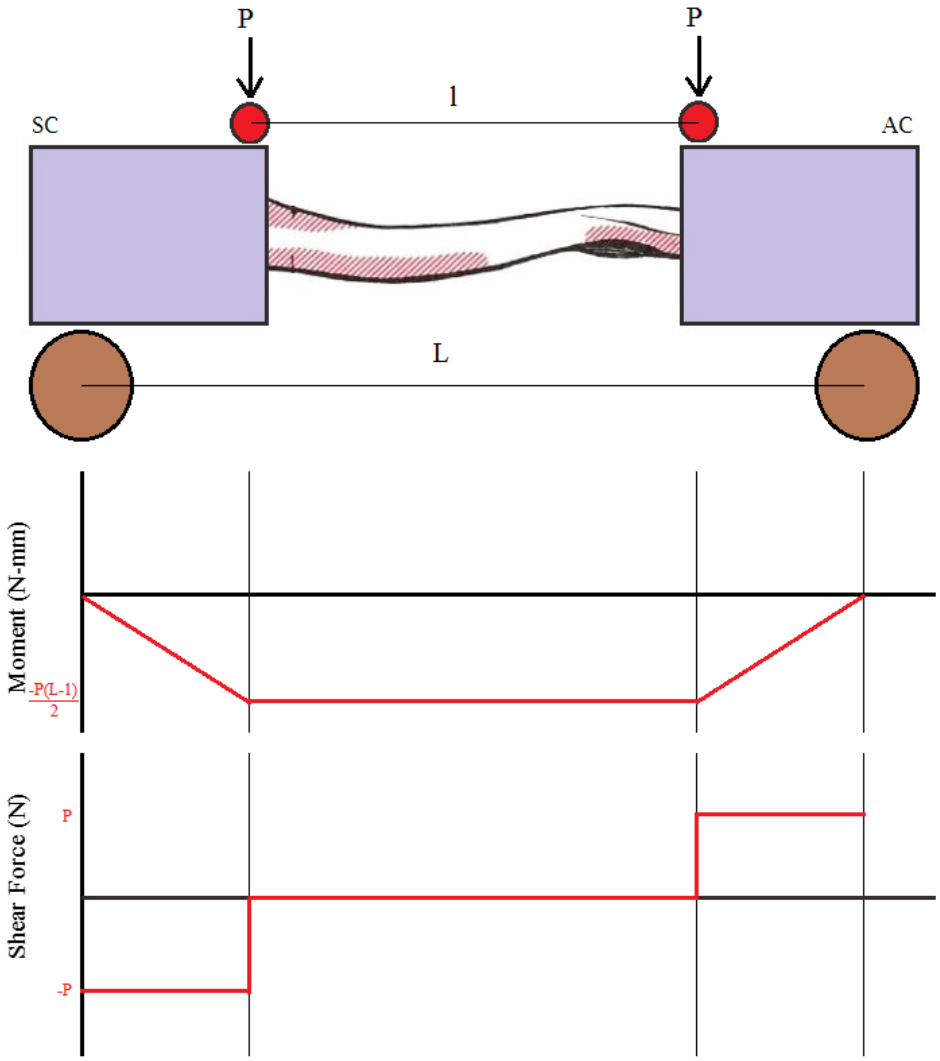

Figure 1.7: *Schematic Drawing of Four Point bending with Moment and Shear Forces Through its Length*

Chapter 2

Literature Review

The main goals of this thesis is to quantitatively compare tunnel configurations for CC ligament reconstruction using four-point bending, create a finite element model of the clavicle to numerically analyze the CC reconstruction techniques and compare with the experimental results. These goals are not unique. In fact, they have been achieved by Li et al, all be it for a different purpose, which was predicting injury to the clavicle in an vehicular accident. Li et al created a FEA clavicle model that could accurately predict response and bone fracture under axial and three point bending loads [13]. The experimental and numerical results showed a high correlation [13], thus deeming their attempt a success.

Experimental testing has also been used to compare reconstruction techniques for the clavicle. Variations of the bending test have been performed to compare both mid clavicle and CC reconstruction techniques. However, some studies preferred four-point bending because of its constant moment, and zero shears characteristics. Four point bending tests have conducted by two researchers. Dumont et al conducted four-point bending tests while comparing the effects of tunnels in foam clavicles; the results show that the single tunnel slightly edged the double tunnels, but did not show any statistical difference [8]. Partal et al conducted

four point bending tests to study the effects of the location of the plate for midclavicular fracture fixation [16].

Partal's and Dumont's studies not only differ in purpose, but in implementation of the four point bending tests. Dumont chose to use a small four point bending setup that applied moment directly to the clavicle [8]. However, Partal used a bigger the four point bending fixtures that applied a moment onto the entire length clavicle specimen through potted ends [16]. Both tests yielded credible results, but this thesis' bending test closely follow Partal et al's implementation of the four point bending tests.

Potting of clavicles was seen in several biomechanical studies [14, 16, 7]. However, descriptions of the potting fixtures and process were not readily available.

Analysis of the experimental data was also determined through the read literature. Turner and Burr, in their summary of biomechanical principles and testing techniques, provided equations that will be used to approximate flexural stiffness, EI, of the clavicle bone specimens [19]. The FE model was compared to Andermahr et al's measurements of cadaver clavicles for validation [2]. Brassey et al found a correlation between the maximum principal of the FE model and the bending stresses - calculated with classical beam theory - of animal long bones differed by an of average 12% [3]. Therefore, clavicle model's predicted principal stress and the approximated bending stress at the point of failure are also compared to determine correlation.

The masters thesis' experimental and FE analysis were patterned to be in par with current trends in clavicle research. Most of the FE analysis work tends to be focusing on the vehicular accidents, and they are also coupled with experimental analysis[13]. However, most of the literature focusing on testing reconstruction techniques contained only experimental results.

Chapter 3

Materials and Methodology

This thesis analyzes the effects of one 3 mm tunnel and two 6 mm tunnels on the mechanical properties of a Sawbones clavicles. Power analysis, Appendix B.1, was performed and the results predetermined a minimum of ten clavicles in a group would yield statistically relevant results. Therefore, twenty biomechanical clavicles were purchased from 4 generation Sawbones clavicles (Sawbones Inc., Vashon Islands, Washington) for the four point bending test. These clavicles were randomly divided into two groups, of which one had the 3 mm tunnel drilled through them, and the other, the two 6 mm tunnels.

The cortical shell of the Sawbones clavicle is made out of fiberglass, and the cancellous material is polyutherane foam [1]. Figure 9 and Tables 2 and 3 show the clavicles and its dimensions and material properties the clavicle as described by Sawbones [1], respectively. The clavicles' dimensions and material properties were considered while design experimental fixtures.

Steel was selected as the primary material for both the for the four point bending fixture and for the pots. With a elastic modulus of 200 GPa, the deflections experienced by steel parts during testing are minimal. Section 3.1 describes the fixtures built for the experiment and how they were used.

A Sawbones clavicle FE model was also created and used to model four point bending. The FE model creation process and analysis process is discussed in Section 3.2. This section also includes the model's validation process.

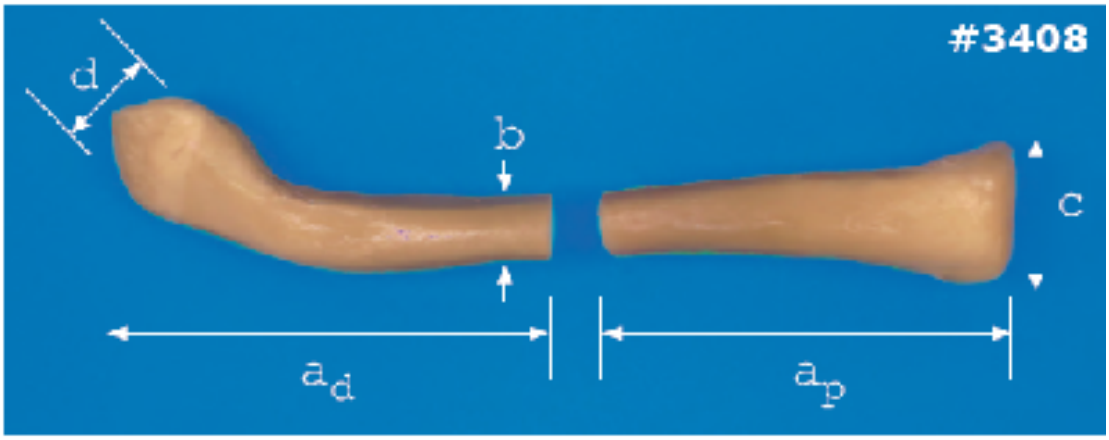

Figure 3.1: *Synthetic Sawbones Clavicle [1]*

Table 3.1: *Physical and Material Properties of Sawbones Clavicle [1]*

Properties		Dimensions
Length	a_d	95 mm
	a_p	80 mm
	b	15 mm
	c	28 mm
	d	29 mm
Elastic Modulus	Cortical Bone	10 GPa
	Cancellous Bone	.155 GPa

3.1 Experimental Analysis

The experimental analysis was performed on the MTS servohydraulic machine (Model 311.31, Eden Prairie, Minnesota) in the Advanced Composite Laboratory at Western Michigan University. Figure 10 shows the schematic drawing of the four point bending fixture with a potted clavicle.

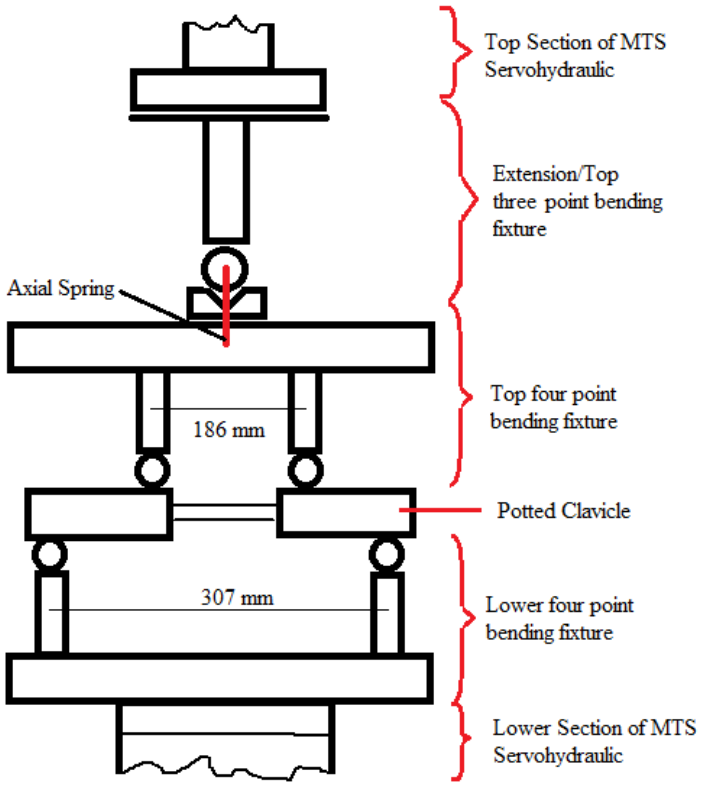

Figure 3.2: *Schematic Drawing of the Four Point Bending Fixture on the MTS Machine*

3.1.1 Potting Fixture and Technique

A potting fixture was also built to improve the accuracy and repeatability of the potting process. This fixture ensured that all the potted clavicles were approximately the same length, and were potted in the same orientation. The pots were made out of steel tubing. These pots prevented failure at either end, and increased the effective length of the clavicle. The pots used measures 39 mm by 39 mm by 104 mm. Approximately 10 mm of clavicle was potted at each end. Therefore, the effective length of the clavicle by approximately 188 mm.

The potting fixture comprised of two blocks of wood that were strategically placed in the fixture to suspend the clavicle so that the acromial and sternal ends could fit when the pots were slid into place horizontally. The potting fixture also

(a) Without Clavicle (b) With Clavicle

Figure 3.3: *Potting Fixture*

had stops put in place to ensure that same amount of clavicle was potted every time. Figure 3.3 shows top views of and empty and loaded potted fixture.

Polymethylmethacrylate (PMMA)(Fricke Dental, Streamwood, Illinois) was used to hold the clavicle in place in the pots. A small amount cement was mixed according to instructions given by the manufacturer and poured in a vertical pot, which was sealed at the bottom with a block of wood. A clavicle was then held in place on the potting fixture, and then inserted into the vertically standing pot with cement – starting with the sternal end and finishing with the acromial end – and held in place until the cement cures. The cement hardened after approximately 2 minutes, in which time the fixture was placed horizontally for the remainder of the curing process. The entire curing process lasted approximately 15 minutes. The pot is then filled with cement after curing is complete.

3.1.2 Drilling

The tunnels were drilled into the clavicles by Dr. Andrew Geeslin after all the sternal ends were potted. A custom guide with the preset holes for the single and double tunnels was developed to fit on the existing potting fixture. Therefore creating an accurate, repeatable drilling process. The single tunnels had a diam-

eter of 3 mm and the two tunnels' diameter was 6 mm, consistent with accepted surgical techniques.

3.1.3 Experimental Setup and Procedure

The potted clavicles were alternated while testing, starting with a one-tunneled clavicle and then two-tunneled one. Alternating the clavicles introduced randomness into the testing, and distributed the risk of test failure between the two groups. This ensures the high quality of the statistical results. Experiments performed by Dumont et al did not find a significant variation in the clavicle's failure loads when a tenodisis screw was insert in the tunnels [8]. Therefore, leaving the tunnels empty was deemed sufficient for this experiment.

After the four-point bending fixtures was loading on the MTS machine, it was aligned and the MTS calibrated. The height of the top fixture was then adjusted to leave just enough allowance to fit in the potted clavicle. The clavicle was then placed onto the bottom fixture, with the outer portion of the pots resting on the anvils. Figure 3.2 shows this set up when all four anvils are in contact with the pots, which occurs approximately 2 mm below the zero setting. The top fixture was lowered at a constant displacement rate of 5mm/min and the clavicle was loaded until failure.

The effective bending stiffness, EI, of the clavicle was estimated using Equation 3.1, where a, L, d and F are the moment arm, outer length of the lower fixtures the displacement, and the applied load. One pitfall of this stiffness approximation it eliminates the influence of inertia cross sectional area, which is an important factor when approximating stress.

$$EI = \frac{F}{d}a^2(\frac{L}{4} - \frac{a}{3}) \tag{3.1}$$

3.2 Finite Element Analysis

Creating an accurate clavicle model is necessary to gain reliable FEA results. Magnetic Resonance Imaging (MRI) or Computed Tomography (CT) data is commonly used to create FEA models for bone [5]. A unique method, referred to as slicing, was utilized to create the clavicle model. Instead of using an MRI or CT scan of the bone, the synthetic sawbones clavicle was sliced transversely for sequential shortening by 1 millimeter at a time. The resulting cross section was then photographed after each slicing.

The cross section images were transferred into Slicer 3D (Havard, Cambridge, Massachusetts) and merged to generate a triangulated surface model of the clavicle by Professor Peter Gustafson. The model was then exported into Hypermesh for further mesh improvements. The triangulated surfaces were improved and used for 2nd order tetrahedral element generation.

The FE model was then used to simulate the four-point bending of a potted clavicle, consistent with typical biomechanical testing procedures. In the FE analysis, the acromial and sternal ends of the clavicle were constrained by rigid beam elements. The beam elements simulated the pots at each end of the clavicle. The sternal end of the clavicle was fixed and the moment was applied in the acromial end end. Figure 3.4 shows a 100 Nmm moment and boundary conditions applied on a clavicle model with two 6mm tunnels. The loading and boundary condition remained the same for the rest of the models.

3.2.1 Geometric Validation

The FE model that was produced through the slicing method was validated before it was used for analysis. Andermahr et al average measurements of 196 clavicles – 90 male and 106 female [2] – were used as a benchmark for the clavicle model.

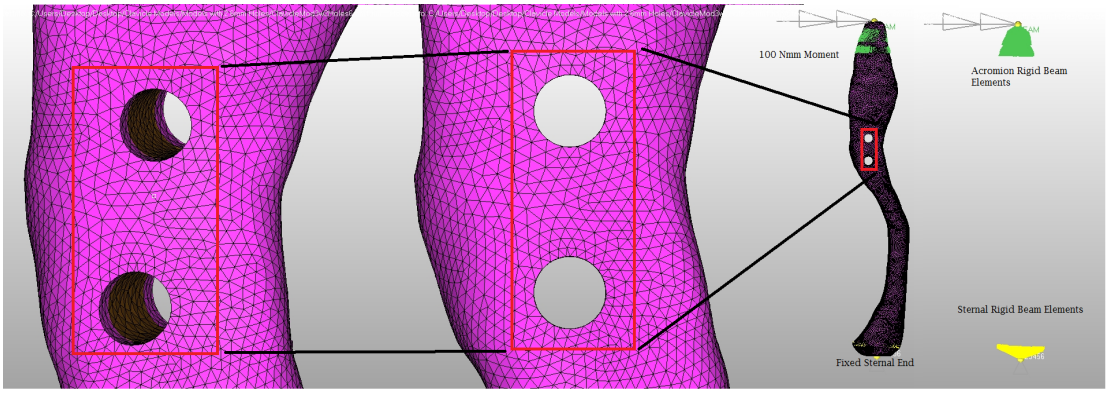

Figure 3.4: *Mesh, Load and Boundary Conditions of the Clavicle with Two 6mm-Tunnels*

These measurements are divided and discussed in two subsequent subsections: peripheral dimensions and cortical thickness.

Table 3.2: *Comparison of Andermahr's Clavicle Measurements to FE Model*

Descriptor	Measurements (cm)	
	Andermahr	FE Clavicle
Length (S1)	15.1 ± 1.1	21.935
Middle Third diameter (S4)	1.2 ± 0.2	1.331
Medial curve depth (S5)	1.7 ± 0.3	2.305
Medial Curve Radius (R1)	7.1 ± 1.3	8.572
Lateral Curve Depth (S6)	1.2 ± 0.3	1.251
Lateral Curve Radius	3.9 ± 1.4	6.173

Peripheral Dimensions

There were 8 characteristic dimensions of the clavicle that were measured and averaged. Andremahr et al measured the length, sternal, middle third and acromial diameters, the medial curve depth and radius, and lateral curve depth and radius of cadaver clavicles [2]. The results from the Andremahr study relevant to this research are summarized in Table 3.2.

Some of the same measurements were taken for the clavicle model with the exception of the acromial diameter and the sternal diameter. These two measurements are not considered because the clavicle is potted and one can visually

detect the error on the acromial end. A comparison of the other dimensions will help with ensuring that there are no errors in the center region of clavicle, which is an important region for the FE analysis. Table 3.2 also summarizes dimensions from the FE model. Both, the FE dimensions and Andermahr's averages, sets of data were then normalized their respective lengths and summarized in Table 3.3. The normalized data shows that the FEA model is within the range of the cadaver clavicle measurements.

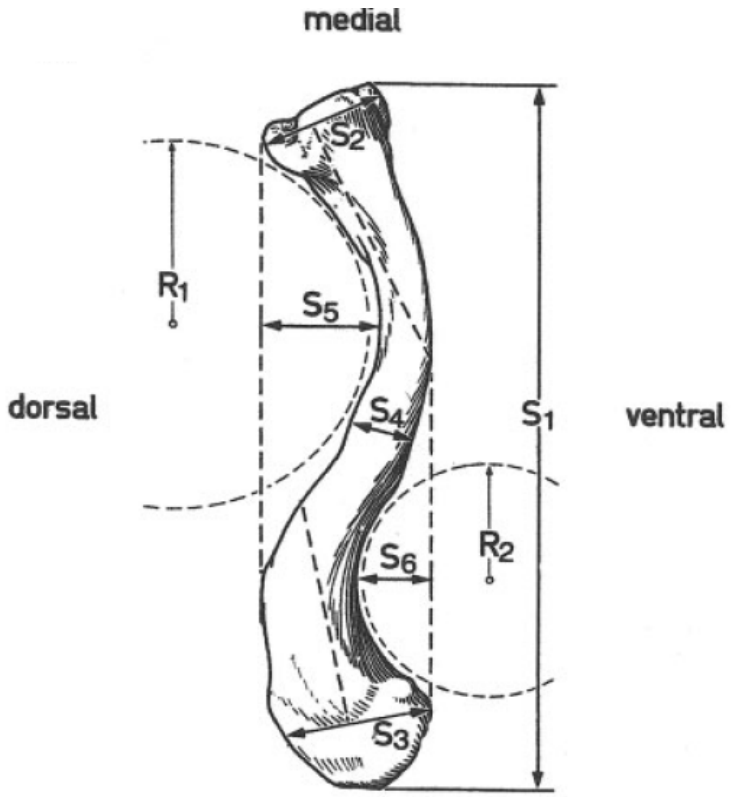

Figure 3.5: *Peripheral Measurements on Clavicle [2]*

Cortical Thickness

Andermahr et al also measured and averaged cortical thickness at seven locations – at 15%, 25%, 33%, 50%, 66%, 75%, and 85% of the clavicle length [2]. Similar measurements were taken at approximately the same locations on the clavicle

Table 3.3: *Comparison of Normalized Andermahr's Clavicle Measurements to FE Model [2]*

Descriptor	Measurements	
	Andermahr	FE Clavicle
Length (S1)	1 ± .0728	1
Middle Third diameter (S4)	0.0795 ± 0.0132	0.0607
Medial curve depth (S5)	0.113 ± 0.0199	0.105
Medial Curve Radius (R1)	0.470 ± 0.0861	0.391
Lateral Curve Depth (S6)	0.0795 ± 0.0199	0.0828
Lateral Curve Radius	0.2583 ± 0.0927	0.281

model to analyze the model shows a similar trend.

Eight equidistant points were picked around each cross section and the cortical thickness was measured using Hypermesh (Altair, Troy, Michigan) tools. The normalized thicknesses are recorded in Table 3.4 and are compared to Andermarhr et al's measurements. The model of showed the same trend until the 85% location, which is in the acromial end region. The data from the model's thickness study and peripheral dimensions will be used to locate appropriate drilling points in the model.

Table 3.4: *Comparison of Normalized Andermahr's Cortical Thickness Measurements to FE Model*

Descriptor	Measurements	
	Andermahr	FE Clavicle
15%	0.524 ± .0952	0.876
25%	-	0.88
33%	-	1
50%	1 ± 0.143	0.966
66%	-	0.0828
75%	-	0.742
85%	0.476 ± 0.190	1.15

3.2.2 Convergence Study

A convergence study of the mesh was performed to ensure good quality. This helped determine the minimum number of elements around the tunnel holes that

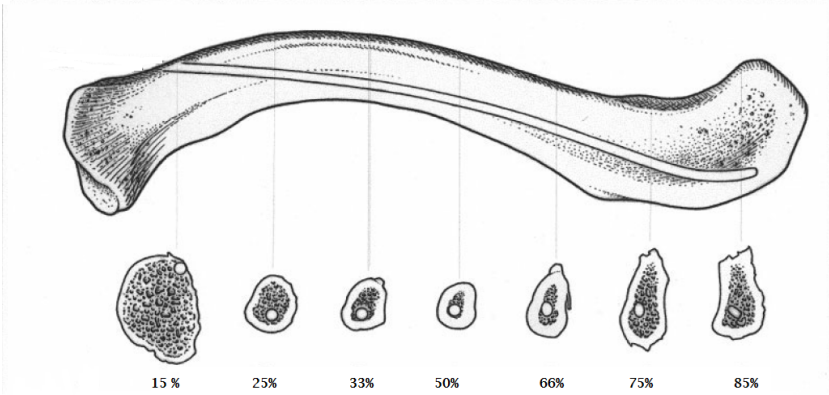

Figure 3.6: *Cross-sectional Area of Clavicle [2]*

were needed to get accurate results. All models were subjected to a 100 Nmm moment applied on the acromial end end of the clavicle while the sternal end remained fixed.

Elements around a 4 mm diameter hole were refined by decreasing their size for five iterations. These refinements were also performed on a hole in a 20 mm–by–20 mm square plate to show the effect of decreasing element size on the mesh density around the hole. Figure 3.7 shows the element sizes used for the convergence are, from coarse to fine, 1.5, 0.75, 0.5, 0.3, and 0.25. These sizes corresponded 8, 17, 25, 42, and 50 elements around the 4 mm diameter hole.

The clavicle was meshed with C3D10 tetra elements. A convergence study was performed with these elements and was stopped when the Von Mises stress had an error of less than 1%. Figures 3.8 a and b shows the Von Mises stress and percentage error after every iteration after the first iteration.

3.3 Comparative Analysis

Two criteria were set to compare the experimental and FE analysis data were to each other. The location of the maximum principal stress and the maximum Von Mises stress on the FE model were compared to the failure location of on synthetic

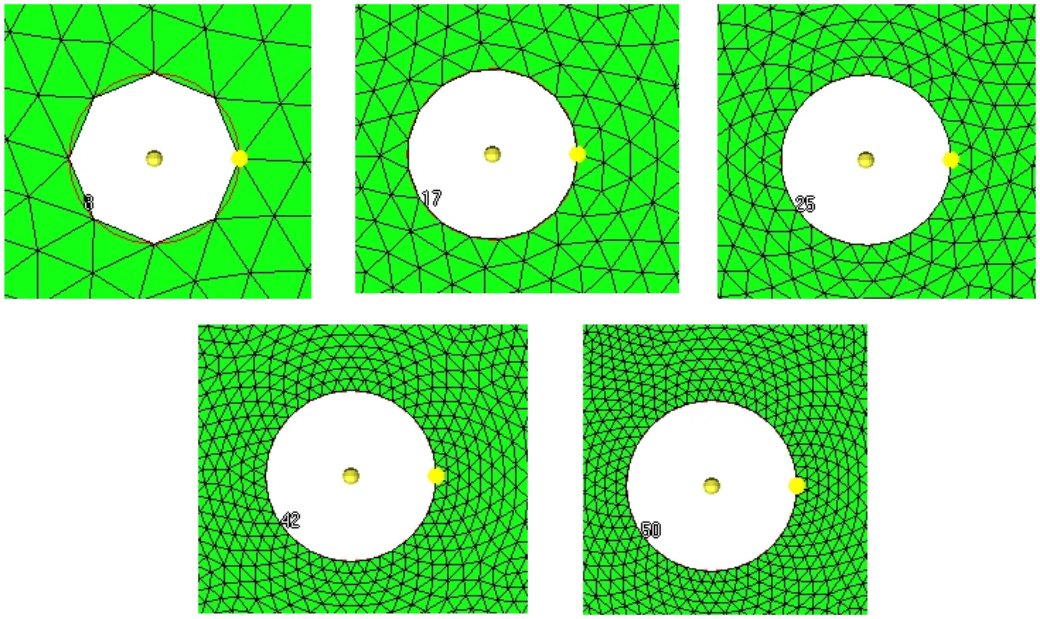

Figure 3.7: *Mesh Density*

clavicles. The bending stress of the clavicle was approximated at the location of failure and compared to the principal stress [3]. The cross section of the clavicle at the point of failure was approximated by ellipse, and its inertia, I_x. The Inertia is calculated using Equation 3.2, where a and b are horizontal and vertical radii of the ellipse respectively. The bending stress was then calculated using Equation 3.3.

The approximated inertia, I_x, was also multiplied by the clavicle's Elastic Modulus to derive another bending stiffness approximation. This approximation was compared to the stiffnesses calculated from experimental data to determine correlation.

$$I_x = \pi \frac{ab^3}{4} \tag{3.2}$$

$$\sigma_{bending} = \frac{My}{I_x} \tag{3.3}$$

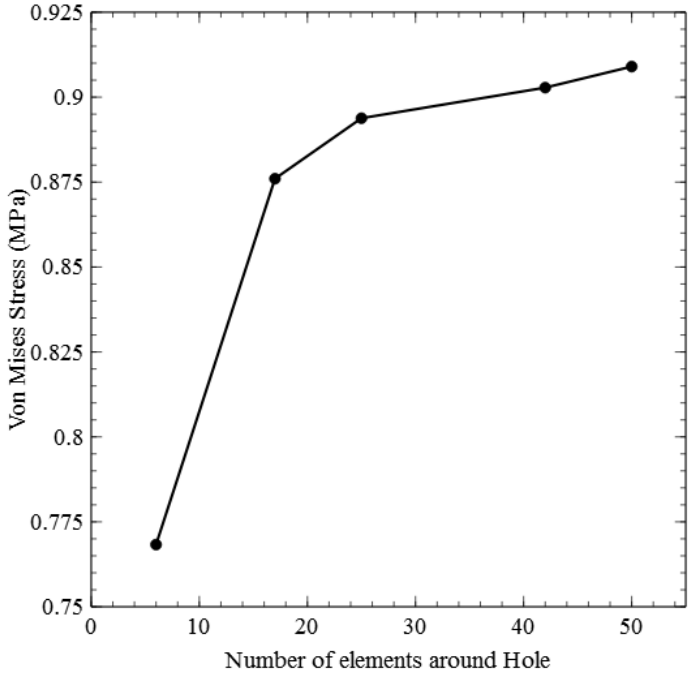

(a) Mesh Convergence of C3D10 Elements

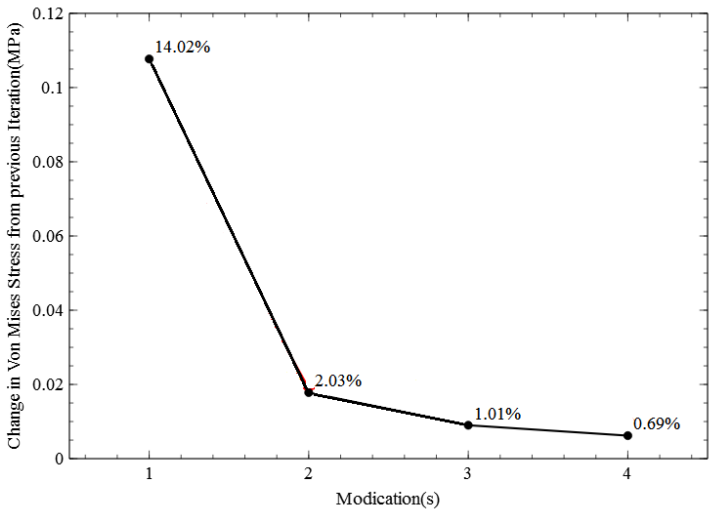

(b) Percentage Error

Figure 3.8: *Maximum Von Mises Stress with Increasing Mesh Density*

Chapter 4

Results

4.1 Experimental Results

The displacement and input force, transmitted through the top section of the four point bending fixture, was recorded during tests at a rate of 102 samples per second. A single test lasted approximately 90 seconds for clavicles with one tunnel, and approximately 60 seconds for clavicles with two tunnels. All the specimens failed at the tunnels. The clavicles with the two 6mm tunnels medial tunnel.

A Python algorithm was developed to retrieve the maximum failure loads, the maximum displacements, and plot the load-displacement curve of each data set. The text file of results were then analyzed in R, an open source statistical package. The t-test have p-value, B.1, less than 10^{-5}, which implies that there was a significant difference between the two groups. The clavicles with one tunnel averaged failure loads of 686 $\pm$ 45.2 N, while clavicles with two tunnels averaged 390 $\pm$ 31.7 N. A box-and-whisker plot that shows the range of the failure loads, Figure 4.2 a, and scatter plot of that relates the failure loads to their maximum displacements, Figure 4.2 b, were both created to visualize the experimental data.

The four point bending fixture had inner length of 186 mm and an outer length,

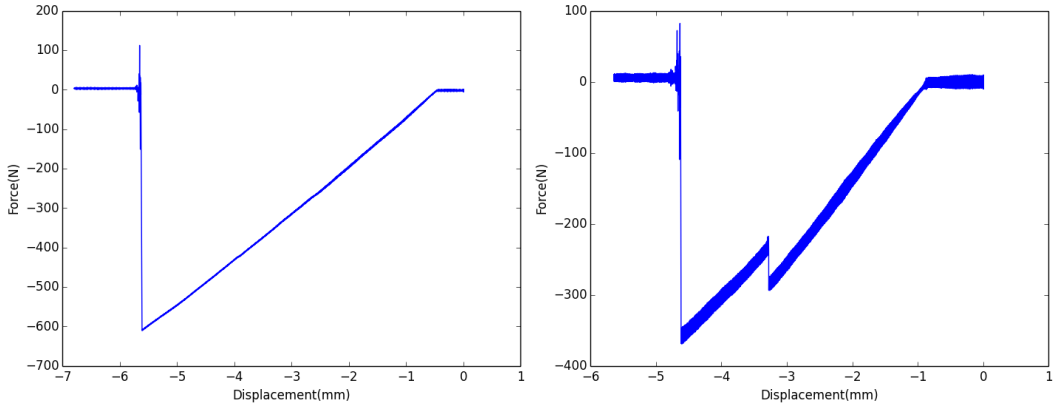

(a) One 3-mm Tunnel (b) Two 6-mm Tunnels

Figure 4.1: *Load-Displacement Curves from Raw Data*

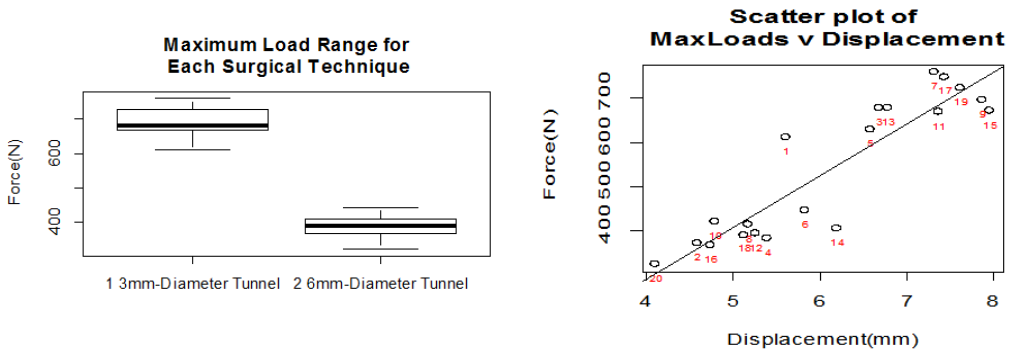

(a) Box-and-Whisker Plot of Maximum Loads(b) Scatter Plot of Maximum Loads and Displacements

Figure 4.2: *Maximum Von Mises Stress with Increasing Mesh Density*

L, of 306 mm. Using these lengths, the moment arm, a, was calculated to be 60.5 mm. The maximum load and displacement were used as F and d, respectively. These values were used in Equation 3.1 to calculate the effective bending stiffness of the clavicle specimens. The results show, Figure 4.3, that the specimens with single tunnels were stiffer, and therefore stronger, than the ones with two tunnels. The single tunnel specimens averaged a stiffness 19.9 $\pm$ 1.55 Nm^2, while the two tunnel specimens had an average stiffness of 15.8 $\pm$ 1.18 Nm^2.

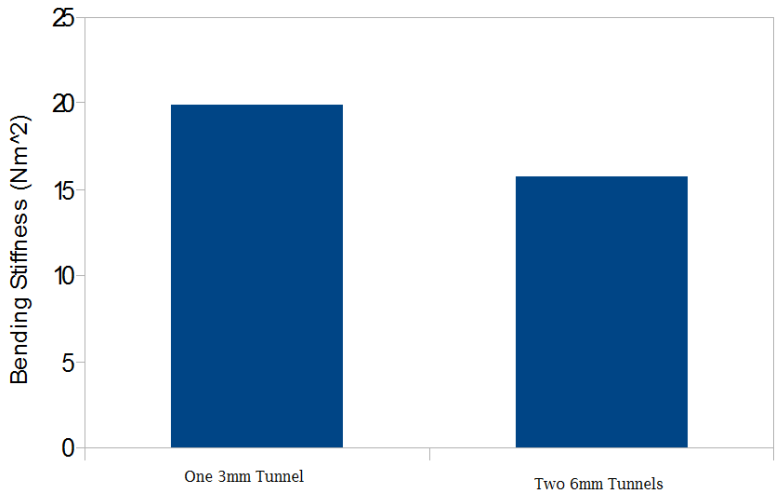

Figure 4.3: *Bending Stiffness Calculation Results*

4.2 Finite Element Analysis Results

The locations of the maximum Von Mises and Principal stresses were compared to the failure location of the clavicle specimens. Both stresses for the single tunnel model were at the approximate location that was observed in experiments. The maximum Principal stress of two-tunneled model, Figure 4.4, correlated with the failure location observed in experimental analysis. However, the two tunneled model predicted the maximum Von Mises stress, Figure 4.5, was at the lateral tunnel.

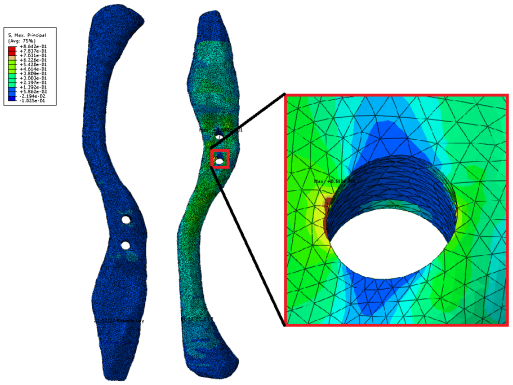

Figure 4.4: *Principal Stress on Two-Tunneled 6mm Clavicle Model*

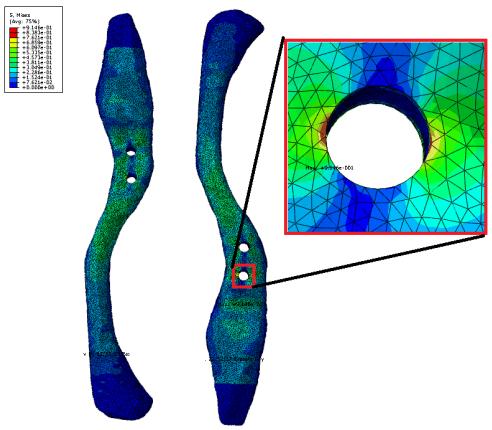

Figure 4.5: *Von Mises Stress on Two-Tunneled 6mm Clavicle Model*

4.3 Comparative Analysis Results

The moments of inertia of both the one and two tunnel failure locations were determined empirically by measuring the clavicles' vertical and horizontal radii and using them in Equation 3.2. These inertias were used in Equation 3.3 to approximate the bending stresses. Table 4.1 shows the calculated bending stress compared to the principal stresses and their relative errors.

The approximated inertias were also multiplied to the elastic modulus, E, of synthetic bones as another way to calculate the bending stiffness. This new stiffness values were found to be relatively close to the ones calculated in the experimental section, Section 4.1. Table 4.2 compares the results and their percentage differences.

Table 4.1: *Principal Stress Compared to Calculated Bending Stress*

Model	FEA Max Principal Stress (MPa)	Calculated Pure Bending Stress (MPa)	% Difference
One tunnel Clavicle	0.909	0.687	24.4%
Two tunnel Clavicle	0.864	0.562	35%

Table 4.2: *Bending Stiffness Calculation Comparison*

Model	$(EI)_{Experimental}$ (Nm^2)	$(EI)_{Area}$ (Nm^2)	% Difference
One tunnel Clavicle	19.9	8.73	56.1%
Two tunnel Clavicle	15.8	13.1	17.1%

Chapter 5

Discussion

The clavicle's unsymmetrical geometry introduces complexities when analytically comparing the surgical techniques. Experimental testing and Finite Element Analysis were used as alternatives to compare single and double tunnel coracoclavicular surgical techniques. In this study, the diameters of the single and double tunnels were 3 and 6 mm respectively. The comparison shows that clavicles with one 3 mm tunnel were determined to be stronger and stiffer than clavicles with two 6 mm tunnels. The assumptions will be discussed further in this chapter.

5.1 Experimental Analysis

The main activities of the experimental process of the study were: creating the fixtures required, testing and the analysis that ensued. The potting and bending fixtures were used multiple times to ensure processes were precise and repeatable, and were deemed satisfactory. All the pots were cut to be same length to within one millimeter. This difference in length may propagate to the potted clavicles' lengths, changing it by $\pm$ 2 mm, and a deviation of $\pm$ 1 mm to moment arm. These deviations in length were too small to affect the general location of clavicle that still remained in the region of constant moment.

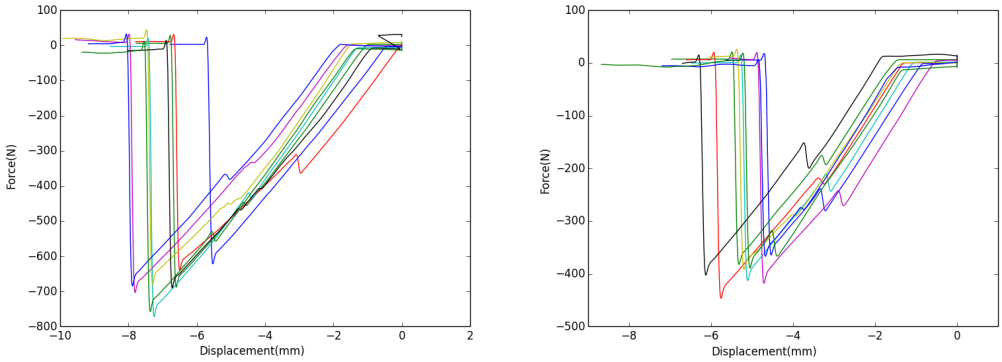

(a) One 3-mm Tunnel (b) Two 6-mm Tunnels

Figure 5.1: *Fitered Load-Displacement Curves*

The bending stiffness, EI, was approximated with two different methods: First, by Equation 3.1 [19], which was derived from Euler-Bernoulli beam theory for four point bending. Using this equation assumed linearity of the load-displacement curves. The second: approximated the local bending stresses to compare with the stresses calculated through Finite Element Analysis. The inertias approximated in this method were multiplied to clavicle's Elastic modulus, thus calculating the second bending stiffness. The approximation and results are discussed further in Section 5.3.

Figures 5.1,a and b, show the aggregated plots of the experimental results.

5.2 Finite Element Analysis

A new approach of creating a Finite Element model of the clavicle, referred to as slicing in this paper, was implemented. The slicing process involved the manual labor of grinding a synthetic clavicle and photographing the cross section, a millimeter at time. The process introduced human errors to the attempt of creating the clavicle model. This error is evident in the Finite Element model that appears to have an unusually longer acromion. Therefore, a validation process

was proposed and implemented on the clavicle model. Using Andemahr et al's clavicle measurements [2], it was shown that even though the length of the clavicle was amiss it possessed comparable curvature and cortical thickness. Also, the additional length was considered a non factor since most of can be modeled as potted.

Both clavicle's material, loading and boundary conditions were simplified in the thesis to reduce computation time. The clavicle model's material properties of the cortical and cancellous bones were assumed to be isotropic. Anisotropy of bone is has been recorded [10, 13], but using Sawbones clavicles allows for the isotropy assumption [1]. The pots were modeled as rigid beam elements and the four point bending was reduced to a cantilever beam with a moment applied to the free end. Both the maximum Von Mises and Principal stress locations were compared to the fracture points observed during testing. It was visually determined that the maximum Principal stress and fracture locations had the best correlation. Von Mises stress was ruled out because the maximum value of the two tunnel model was on the hole nearest to acromion, which differed from the failure location observed for the two 6 mm tunnel clavicle specimens.

Data from the clavicles with two tunnels also hints to the influence of a tunnel's location on the clavicle's strength and rigidity. Qualitatively, it can be deduced that risk of failure increases the more medial the tunnel's location. More analysis and testing would be needed to quantitatively analyze this hypothesis.

5.3 Comparative Analysis

The correlation of the maximum Principal stress and fractures locations, allowed for comparison the principal stress and pure bending stress of the clavicle [3]. The cross section of the fracture location was approximated by a hollow ellipsoid,

Figure 5.2, that best fit it's horizontal and vertical diameters, and with a cortical shell that is 1 mm thick. The percentage differences in the stresses, single tunnel difference of 25% and double tunnel difference of 35%, were greater than Brassey et al's suggested 12% difference. However, this may be attributed to difference in bone geometry of clavicle to the animal tibia and femurs that were the focus Brassey et al's study, and errors in approximating the inertia.

The comparison of bending stiffness calculation methods, Table 4.2, shows the discrepancies in bending stiffness. The two tunnel approximation had the small difference of 17.1% compare to the one tunnels 56.1%. These differences in bending stiffnesses are attributed to overestimation of the cross section area. Even though there are differences, this comparison validates the principal stress approximated in the Finite Element model.

These comparison results show the approach used in the thesis is adequate, but in need of improvements. Comparing displacements was considered, but the difference between the experiment's and FE analysis' boundary conditions were different.

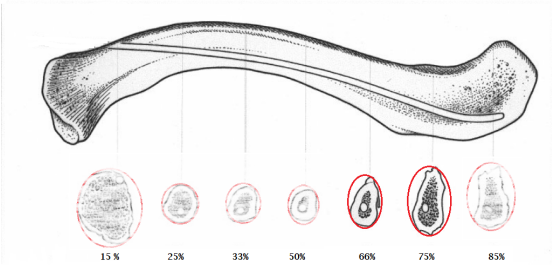

Figure 5.2: *Approximated Ellipsoid at Each Cross Section of Clavicle [2]*

5.4 Future Work

More work needs to be done the clavicle model and the Finite Element Analysis. Creating another clavicle model from MRI or CT data [5, 13]. However, using

a 3D scanner get the cortical shape and then drawing in the cancellous bone using Andemahr's measurements of the cortical thickness may be used as better approach. A more accurate clavicle model would simplify locating tunnel centers on the model. The current tunnel centers were located visually by comparing curvature of the model and synthetic clavicle.

Another improvement that can be performed is creating a model that includes pots and four point bending fixture. Simulating four point bending with the fixtures will help in better approximating the stresses and displacements experienced by the clavicle during testing.

It is also recommended that strain gages should be attached to clavicle specimen during testing. Attaching strain gages has been shown to be a successful way of comparing the stresses and strains experienced by the clavicle to FE analysis results [13]. This would help in validating the stresses and strains observed in the Finite Element models. This will make studying other effects of tunnel more cost effective and quick. Examples of studies that can be done are:

- The effects varying tunnels size
- Determining the optimal distance between two tunnels
- and, Determining how fractures develop through dynamic simulations.

Chapter 6

Conclusion

Findings in thesis show differences in coracoclavicular reconstruction techniques that utilize different size tunnels can be quantified and compared using four point bending. Experimental results show that clavicle with one 3 mm tunnel are stiffer and stronger than the ones with two 6 mm tunnels. These results are similar to Dumont's findings that constrained the diameters of the tunnels. More testing is need to determine the effects of increasing the diameter of the tunnels.

Comparison of the experimental testing and Finite Element Analysis data shows some correlation. The maximum principal stresses in the Finite Element models were in similar regions to the failure locations observed in testing. The bending stress of the clavicle was also approximated analytically and compared to the maximum principal stress recorded in the Finite Element analysis and the values can be used as evidence of the success of the study.

6.1 Contributions

This section highlights and summarizes unique and original contributions in this thesis study.

A robust bending setup capable of performing three and four point bending was

designed and built. The four point bending test was selected as the comparator, but the three point bending fixture was added into the build in case it is needed in future studies. Figure 3.2 shows the schematic drawing of the fixtures and its setup on the MTS servohydraulic machine.

A potting fixture was also built to improve the accuracy and repeatability of the potting process. This fixture ensured that all the potted clavicles were approximately the same length, and in the same orientation. Figure 3.3 show the potting fixture with and without a potted clavicle.

A slicing process was utilized to create the clavicle surface model. This process involved slicing (sanding) off a synthetic sawbones clavicle transversely 1 mm at a time and photographing the resulting cross section after each slicing. The surfaces were used to create an FE model that was validated before it was used for analysis.

The validation process developed compared Andermahr et al average measurements of 196 clavicles – 90 male and 106 female [2] – to the FE model's measurements. This verified that FE model satisfied the geometric characteristics of a clavicle and was deemed good for simulations.

6.2 Recommendations

Based on the results in this thesis and the likelihood of fracture, it is recommended that a surgeon use the single 3 mm Dogbone tunnel whenever possible. If double tunnels is deemed surgically advantageous, the tunnel locations should be carefully considered as their relative location affect stress concentrations and failure risk. Additional research is necessary to determine the factors governing tunnel size and placement. The validated FE model should be exercised as part of that research.

Bibliography

[1] Sawbones Europe Ab. biomechanical catalogue Europe middle east africa.

[2] Jonas Andermahr, Axel Jubel, Andreas Elsner, Jan Johann, Axel Prokop, Klaus Emil Rehm, and Juergen Koebke. Anatomy of the clavicle and the intramedullary nailing of midclavicular fractures. *Clinical anatomy (New York, N.Y.)*, 20(1):48–56, January 2007.

[3] Charlotte a Brassey, Lee Margetts, Andrew C Kitchener, Philip J Withers, Phillip L Manning, and William I Sellers. Finite element modelling versus classic beam theory: comparing methods for stress estimation in a morphologically diverse sample of vertebrate long bones. *Journal of the Royal Society, Interface / the Royal Society*, 10(79):20120823, March 2013.

[4] Paul Celestre, Claire Roberston, Andrew Mahar, Richard Oka, Matthew Meunier, and Alexandra Schwartz. Biomechanical Evaluation of Clavicle Fracture Plating Techniques : Does a Locking Plate Provide Improved Stability ? 22(4):241–247, 2008.

[5] A Chawla, S Mukherjee, and G Sharma. Finite Element Meshing Of Human Bones From MRI / CT Raw Data MRI scan data Interior and exterior Solid model FE.

[6] Dogbone. AC Repair - Dog Bone Button. 2014.

[7] Darren S Drosdowech, Stuart E E Manwell, Louis M Ferreira, Danny P Goel, Kenneth J Faber, and James A Johnson. Biomechanical Analysis of Fixation of Middle Third Fractures of the Clavicle. 25(1):39–43, 2011.

[8] Guillaume D Dumont, Robert D Russell, Justin R Knight, William R Hotchkiss, William a Pierce, Philip L Wilson, and William J Robertson. Impact of tunnels and tenodesis screws on clavicle fracture: a biomechanical study of varying coracoclavicular ligament reconstruction techniques. *Arthroscopy : the journal of arthroscopic & related surgery : official publication of the Arthroscopy Association of North America and the International Arthroscopy Association*, 29(10):1604–7, October 2013.

[9] Adam J Farber, Brett M Cascio, and John H Wilckens. Type III acromioclavicular separation: rationale for anatomical reconstruction. *American journal of orthopedics (Belle Mead, N.J.)*, 37(7):349–55, July 2008.

[10] S A Goldstein. THE MECHANICAL DEPENDENCE PROPERTIES OF TRABECULAR BONE : ON ANATOMIC LOCATION AND. 1961.

[11] Henry Gray. File:gray326.png.

[12] Mark J. Lemos. Evalution and Treatment of the injured acromioclavicular joint in athletes.pdf. *American Orthopaedic Society for Sports Medicine*, 26(1):138 – 144, 1998.

[13] Zuoping Li, Matthew W Kindig, Jason R Kerrigan, Richard W Kent, and Jeff R Crandall. Development and validation of a subject-specific finite element model of a human clavicle. *Computer methods in biomechanics and biomedical engineering*, 16(8):819–29, January 2013.

[14] Augustus D Mazzocca, Stephen a Santangelo, Sean T Johnson, Clifford G Rios, Mark L Dumonski, and Robert a Arciero. A biomechanical evaluation

of an anatomical coracoclavicular ligament reconstruction. *The American journal of sports medicine*, 34(2):236–46, February 2006.

[15] Matthew D Milewski, Marc Tompkins, Juan M Giugale, Eric W Carson, Mark D Miller, and David R Diduch. Complications related to anatomic reconstruction of the coracoclavicular ligaments. *The American journal of sports medicine*, 40(7):1628–34, July 2012.

[16] George Partal, Kathleen N Meyers, Nicholas Sama, Eric Pagenkopf, Paul B Lewis, Ariel Goldman, Timothy M Wright, and David L Helfet. Superior versus Anteroinferior Plating of the Clavicle Revisited : A Mechanical Study. 10021:420–425, 2010.

[17] Brent a Ponce, Peter J Millett, and Jon J.P Warner. Acromioclavicular joint instability—reconstruction indications and techniques. *Operative Techniques in Sports Medicine*, 12(1):35–42, January 2004.

[18] Kimberly a Turman, Chealon D Miller, and Mark D Miller. Clavicular fractures following coracoclavicular ligament reconstruction with tendon graft: a report of three cases. *The Journal of bone and joint surgery. American volume*, 92(6):1526–32, June 2010.

[19] C. H. Turner and D.B Burr. Basic biomechanical measurements of bone.pdf. *Bone*, 14(4):595–608, 1993.

Appendix A

Python Script and Outputs

A.1 Script

C:\Users\Mark\Desktop\ExperimentCode.py Wednesday, September 24, 2014 2:32 PM

```
import os
from numpy import *
from matplotlib import pyplot as plt
from matplotlib.backends.backend_pdf import PdfPages

# Paths to experimental data and output file
path = 'C:\Users\Mark\Desktop\Experimental Data'
path2 = 'C:\Users\Mark\Desktop\CLAVICLE RESEARCH'

# Clears already exist output file
outfile = 'output.dat'
open(outfile,'r+').truncate()

print "Starting to upload data"

# Opens each input file and save the information as 1D arrays
for filename in os.listdir(path):
    file = os.path.join(path, filename)
    outfile = 'output.dat'
    data = loadtxt(file)
    time = data[:,0]
    displacement = data[:,1]
    force = data[:,2]

    # Max force is retrieved from force array and written into output file
    maxForce = max(abs(force))
    for i in range(0,len(force)-1):
        if maxForce == abs(force[i]):
            print displacement[i]
    x = filename[0:len(filename )- 4] + ' Max force is: ' + str(maxForce) +' N'

    outfile = open(outfile, 'a')
    outfile.write(x + '\n')
    print "Plotting..."
    fig = plt.figure()
    plt.plot(displacement, force)
    plt.xlabel("Displacement(mm)")
    plt.ylabel("Force(N)")
    figFile = os.path.join(path,filename)
    plt.savefig(figFile +'.png', bbox_inches = 'tight')



outfile.close()
```

-1-

C:\Users\Mark\Desktop\Thesis Documents\filt.py Sunday, October 26, 2014 2:43 PM

```
import scipy.signal as signal

def filt(x):
    # First, design the Buterworth filter
    N  = 2    # Filter order
    Wn = 0.01 # Cutoff frequency
    B, A = signal.butter(N, Wn, output='ba')

    # Second, apply the filter
    xf = signal.filtfilt(B,A, x)
    return xf
```

A.2 Output

MaxLoads1

SampleNumber	Displacement	MaxLoad	TunnelType
1	5.6119828	610.93604	1Tunnel3mmDiameter
2	4.6003523	369.10269	2Tunnel6mmDiameter
3	6.6825867	677.42157	1Tunnel3mmDiameter
4	5.4026899	381.31158	2Tunnel6mmDiameter
5	6.5822897	628.82196	1Tunnel3mmDiameter
6	5.8276899	444.51007	2Tunnel6mmDiameter
7	7.3281021	759.44922	1Tunnel3mmDiameter
8	5.190176	412.81747	2Tunnel6mmDiameter
9	7.881184	695.51837	1Tunnel3mmDiameter
10	4.7914147	419.52948	2Tunnel6mmDiameter
11	7.3736191	668.5741	1Tunnel3mmDiameter
12	5.2653818	392.70853	2Tunnel6mmDiameter
13	6.7962914	677.90338	1Tunnel3mmDiameter
14	6.2049718	402.86938	2Tunnel6mmDiameter
15	7.9585104	672.30432	1Tunnel3mmDiameter
16	4.7417493	365.9982	2Tunnel6mmDiameter
17	7.4431567	748.93182	1Tunnel3mmDiameter
18	5.1306067	389.11938	2Tunnel6mmDiameter
19	7.6264086	724.45105	1Tunnel3mmDiameter
20	4.1192918	323.32294	2Tunnel6mmDiameter

Figure A.1: Load-Displacement Data from One Tunnel Clavicles

(a) Unfiltered

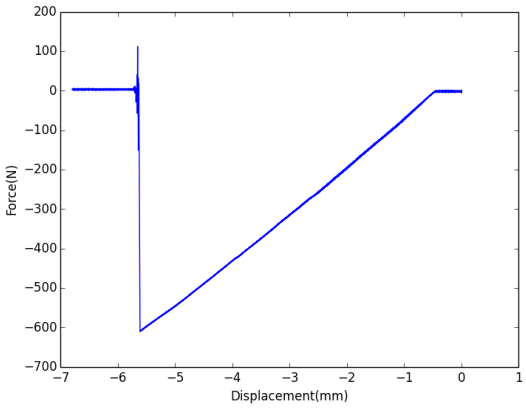

(b) Filtered

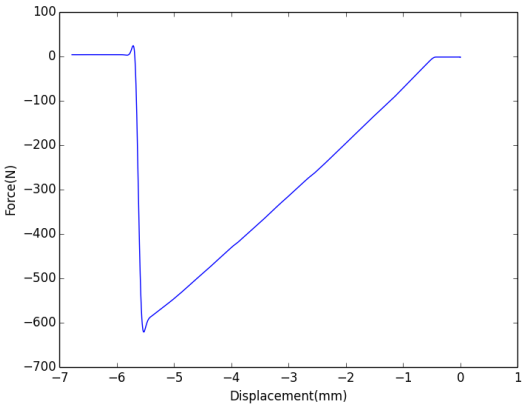

(c) Unfiltered

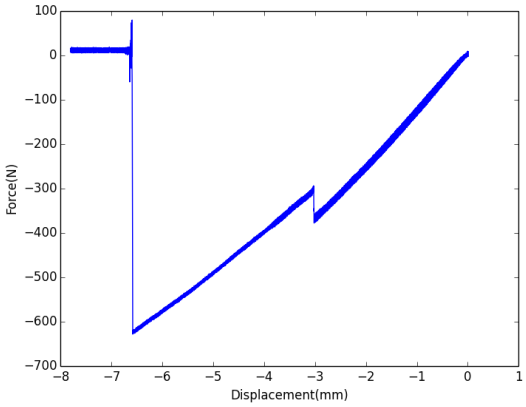

(d) Filtered

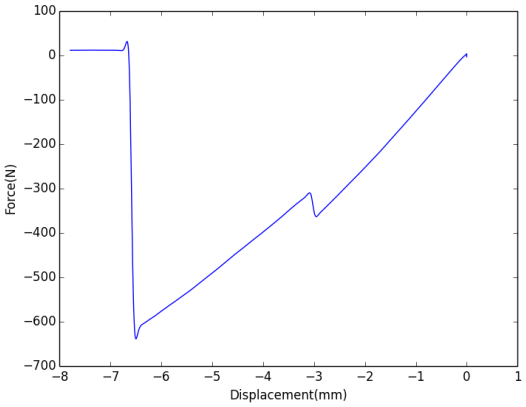

(e) Unfiltered

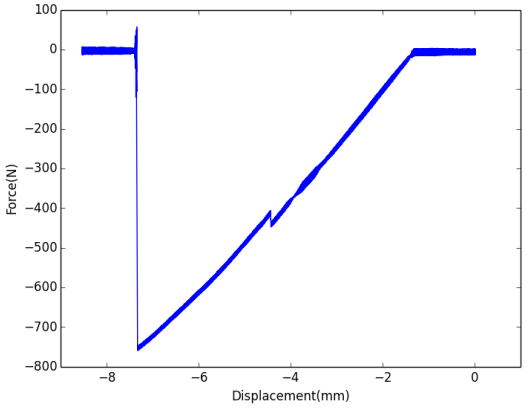

(f) Filtered

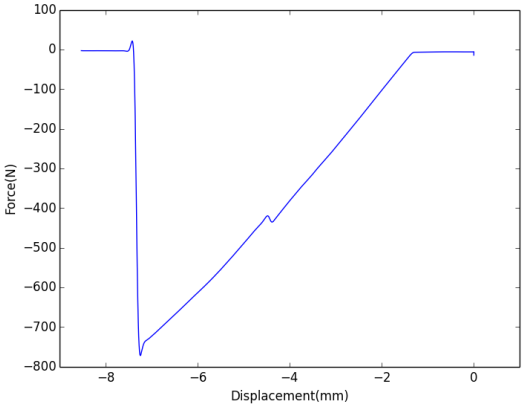

Figure A.2: Continued: Load-Displacement Data from One Tunnel Clavicles

(a) Unfiltered

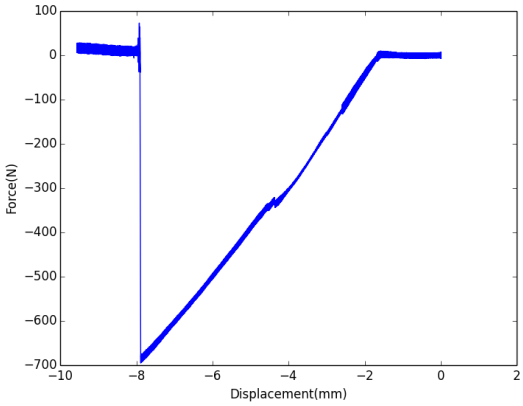

(b) Filtered

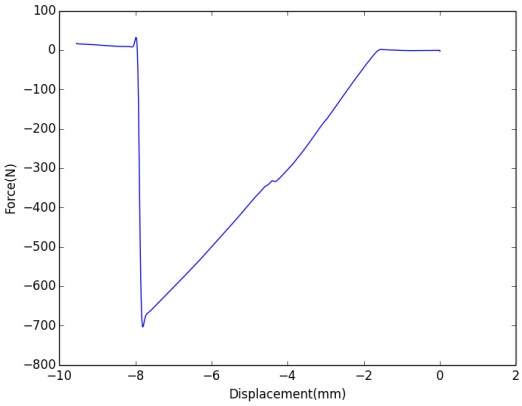

(c) Unfiltered

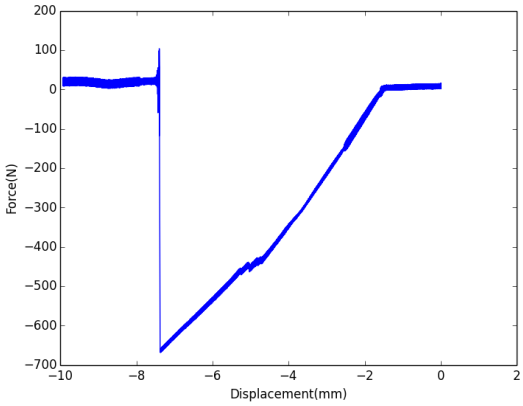

(d) Filtered

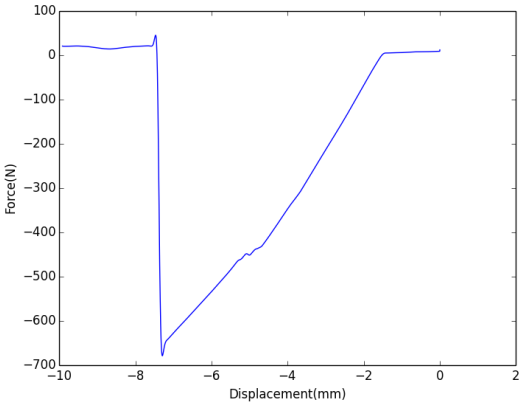

(e) Unfiltered

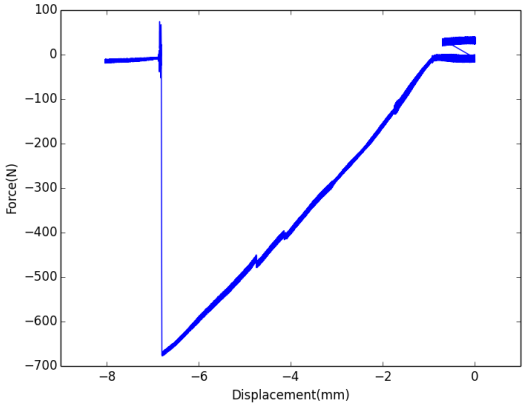

(f) Filtered

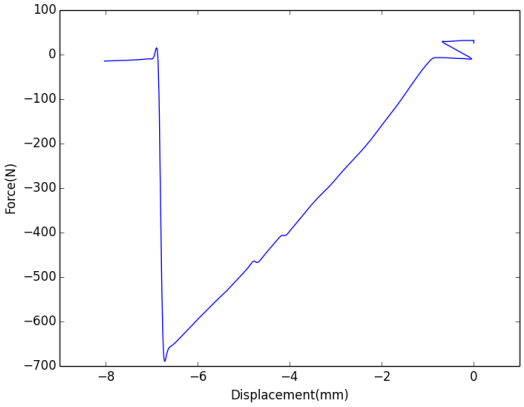

Figure A.3: Continued: Load-Displacement Data from One Tunnel Clavicles

(a) Unfiltered

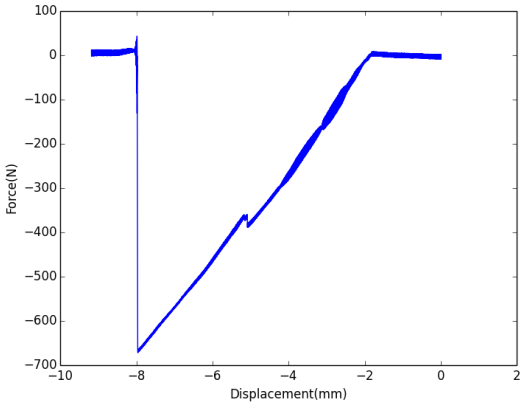

(b) Filtered

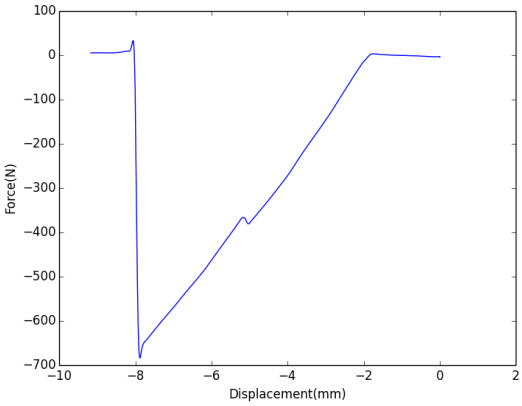

(c) Unfiltered

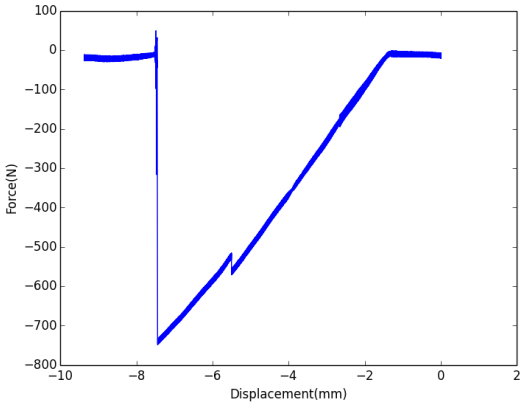

(d) Filtered

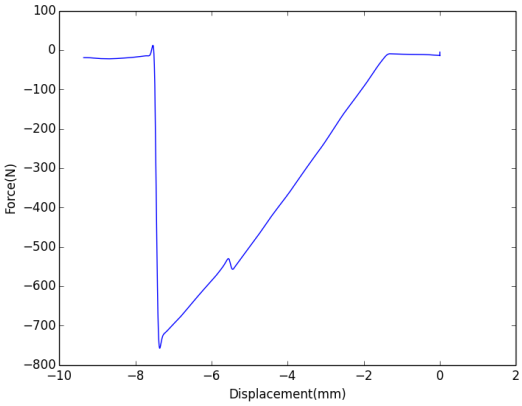

(e) Unfiltered

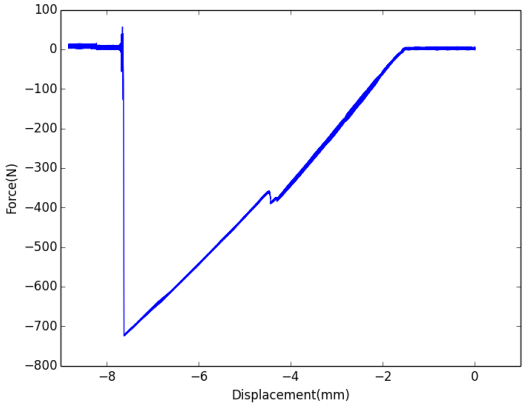

(f) Filtered

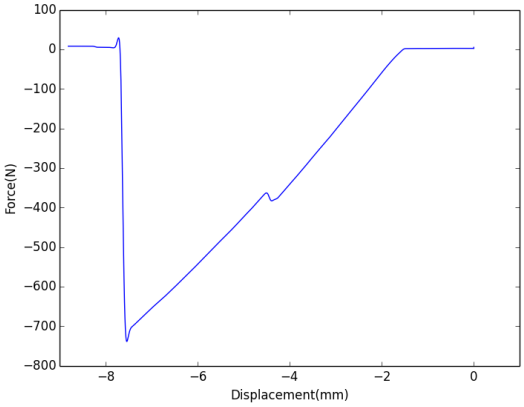

Figure A.4: Continued: Load-Displacement Data from One Tunnel Clavicles

(a) Unfiltered

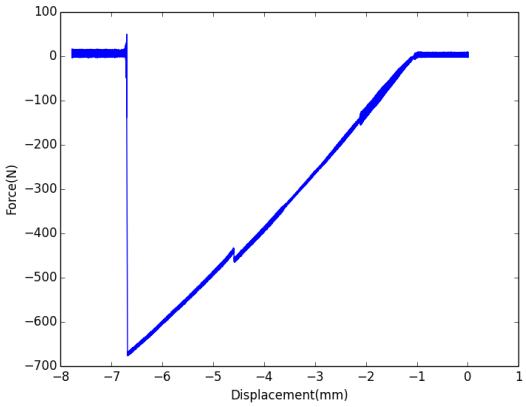

(b) Filtered

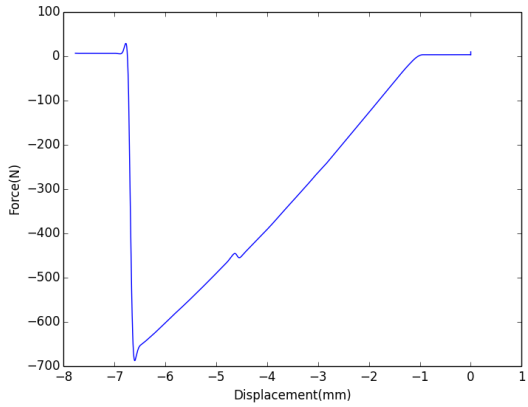

Figure A.5: Load-Displacement Data from Two Tunnel Clavicles

(a) Unfiltered

(b) Filtered

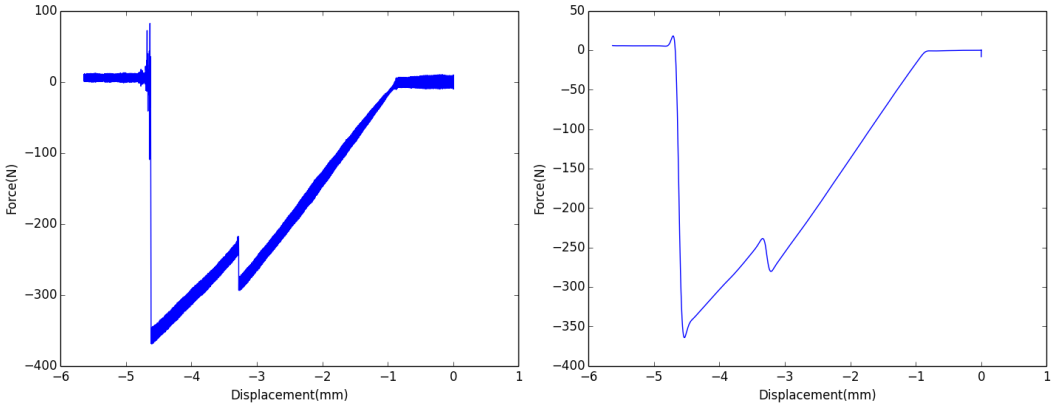

(c) Unfiltered

(d) Filtered

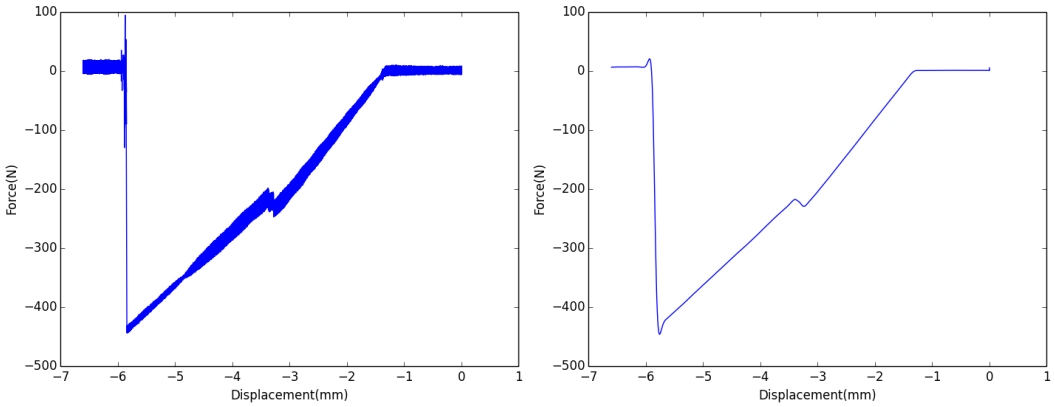

(e) Unfiltered

(f) Filtered

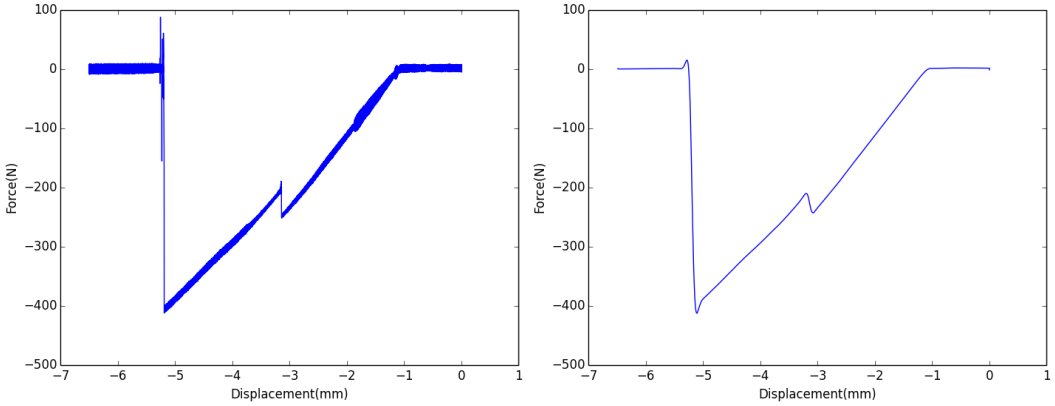

Figure A.6: Continued:Load-Displacement Data frow Two Tunnel Clavicles

(a) Unfiltered

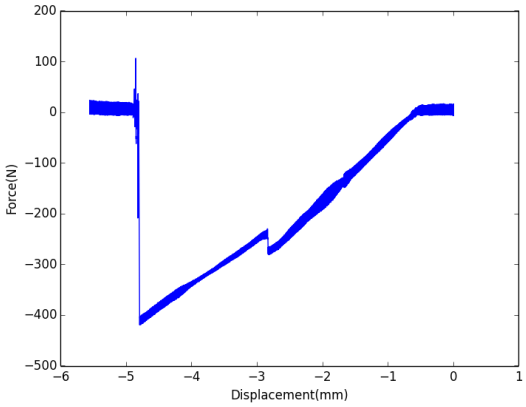

(b) Filtered

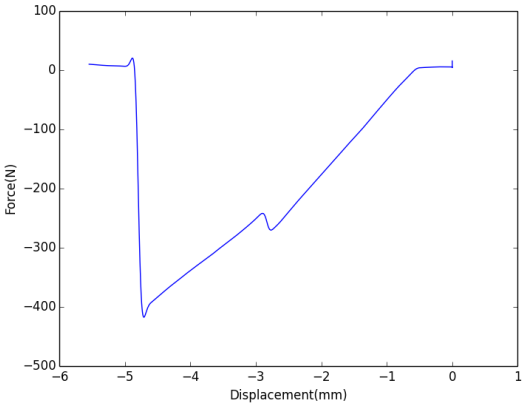

(c) Unfiltered

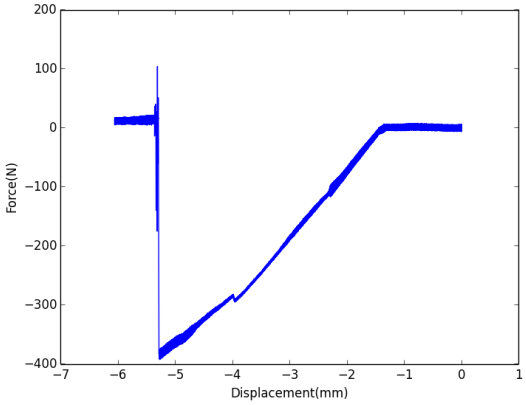

(d) Filtered

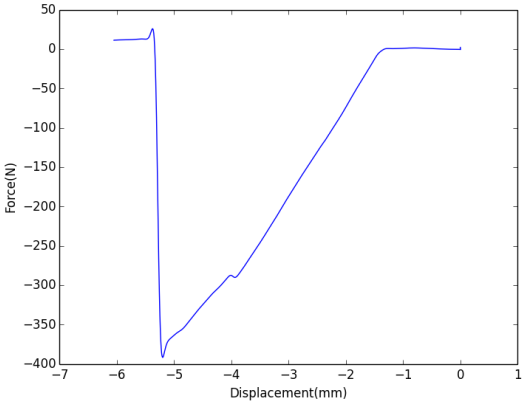

(e) Unfiltered

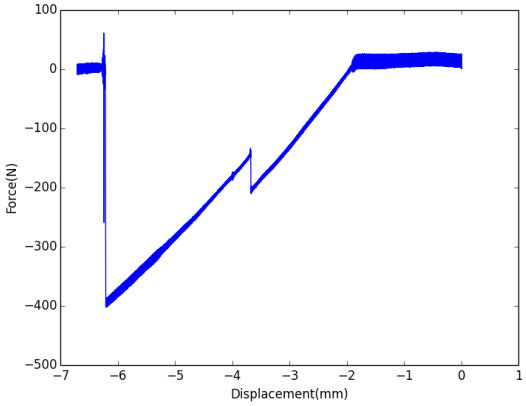

(f) Filtered

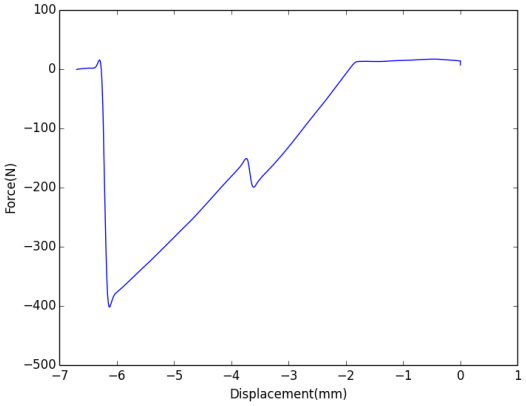

Figure A.7: Continued:Load-Displacement Data frow Two Tunnel Clavicles

(a) Unfiltered

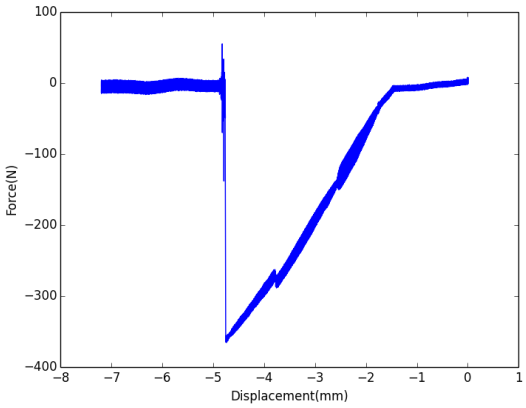

(b) Filtered

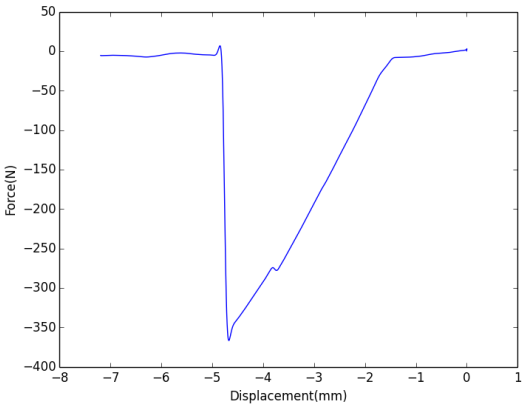

(c) Unfiltered

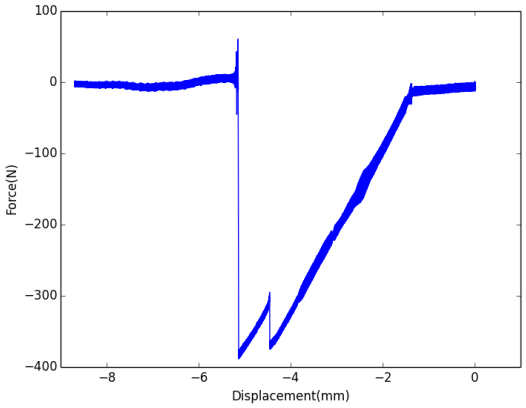

(d) Filtered

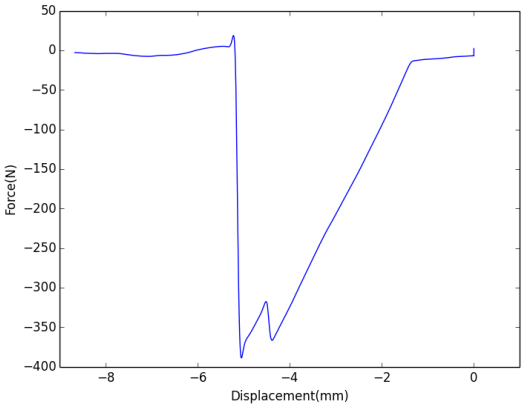

(e) Unfiltered

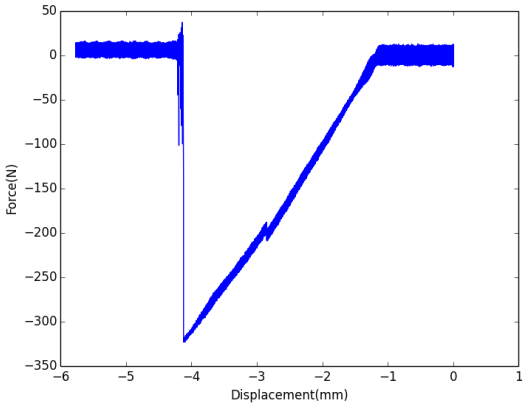

(f) Filtered

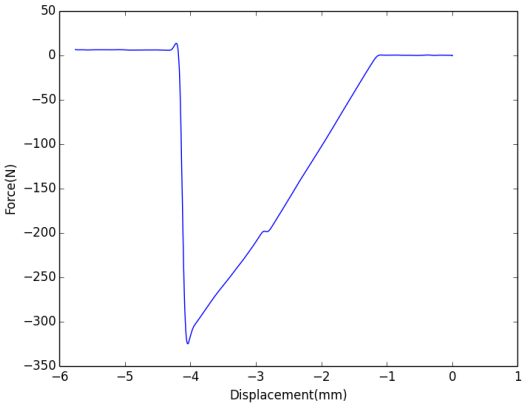

Figure A.8: Continued:Load-Displacement Data frow Two Tunnel Clavicles

(a) Unfiltered

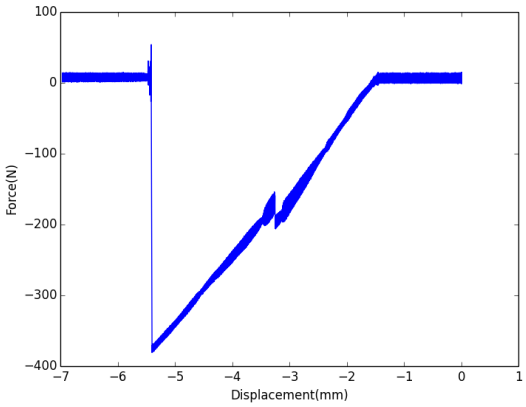

(b) Filtered

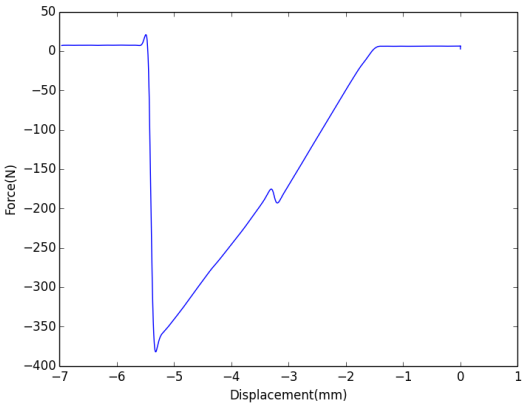

Appendix B

R-Statistics Package Algorithm and Output

B.1 Script


```
##########################################
## Master Thesis Statistical Analysis Code  #
## by Mark Omwansa  #
##########################################

# Read .dat file

expData <- read.table(dataFile, header = TRUE)

# T-test analysis of the two groups

 t.test(expData$MaxLoad ~ expData$TunnelType)

# T-test output

#########################################################################
#Welch Two Sample t-test                                                #
#                                                                       #
#  data:  expData$MaxLoad by expData$TunnelType                         #
# t = 16.0881, df = 16.133, p-value = 2.337e-11                         #
# alternative hypothesis: true difference in means is not equal to 0    #
# 95 percent confidence interval:                                       #
#  257.2850 335.3194                                                    #
# sample estimates:                                                     #
# mean in group 1Tunnel3mmDiameter mean in group 2Tunnel6mmDiameter     #
#                         686.4312                           390.1290   #
#########################################################################

# Box-and-whisker plot

 boxplot(MaxLoad~TunnelType, data=expData, ylab="Force(N)",names = c("1 3mm-Diameter Tunnel","2 6mm-
 title(main="Box-Whisker Plot of Failure Loads")

# Scatter plot

plot(disp,maxLoad,xlab="Displacement(mm)",ylab="Force(N)")
title(main="Scatter plot of\n MaxLoads v Displacement")
abline(lm(maxLoad~disp))
text(disp,maxLoad, row.names(expData), cex = 0.6, pos=1,col="red")
```

B.2 Output

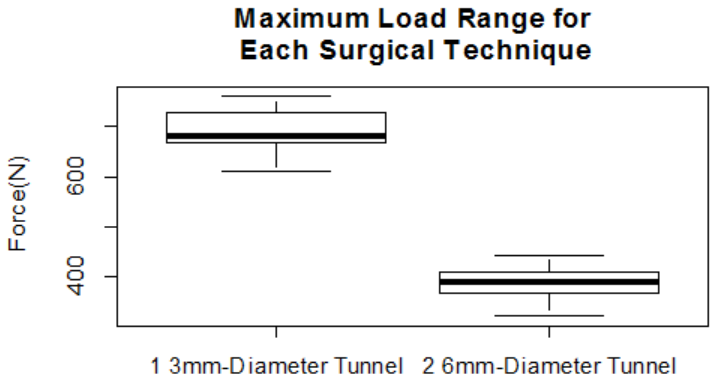

(a) Box-and-Whisker Plot of Maximum Loads

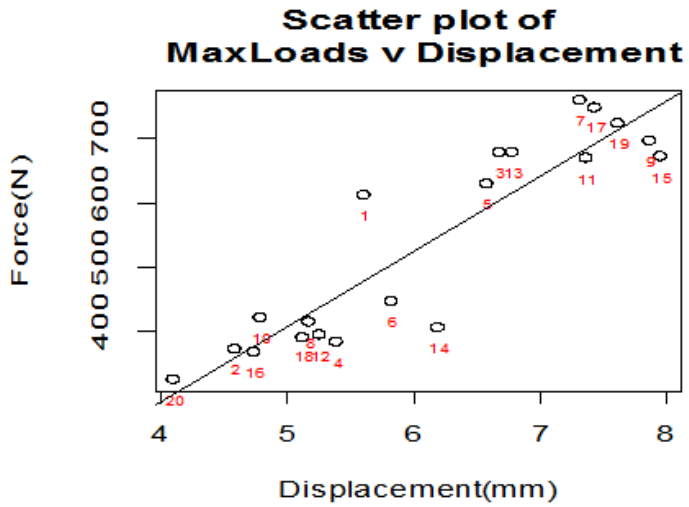

(b) Scatter Plot of Maximum Loads and Displacements

Figure B.1: *Maximum Von Mises Stress with Increasing Mesh Density*